Error indicators for controlling automatic grid refinement in ISIS-CFD

Zaib Ali

Master of Science Thesis
Ecole Centrale de Nantes, France

Supervisor: Dr. Jeroen Wackers

Abstract

This master’s thesis work is a part of the effort to build various error indicators or refinement criteria for the adaptive grid refinement part of the ISIS-CFD flow solver. The purpose is to develop such refinement criteria which respond to the needs of the flow solver users and are general and flexible. Three types of refinement criteria are tested for various flow and refinement conditions. We focus here on the capturing of vortices to observe the performance of refinement criteria. Two test cases are used for this purpose. The work is done on the initial stages and more in-depth analysis of the refinement criteria is proposed in order to use them efficiently.

Acknowledgements

I would like to express the deepest appreciation to Dr. Jeroen Wackers, my thesis supervisor, who has the attitude and the substance of a genius: he continually and convincingly conveyed a spirit of adventure in regard to research during the whole period. Without his guidance and persistent help this dissertation would not have been possible.

I thank Dr. Michel Visonneau, the head of CFD research group at Ecole Centrale de Nantes, who gave me the opportunity to work with his research group. His constant support and encouragement kept me motivated throughout the project.

This work would never have been accomplished without the help of Dr. Patrick Queutey and Dr. Emmanuel Guilmineau. They spent a lot of time guiding me and were always available to help me. I am grateful for their countless help, support, discussion and guidance.

Last but not the least; I would like to express my gratitude to my loving parents, brother and sister for supporting and encouraging me throughout my life.

Table of contents

List of figures

List of tables

.

1 Introduction

In computational fluid dynamics (CFD), one of the challenges has been the accurate predictions of complex flows. Different methodologies have been adapted in order to seek the solutions which have acceptable numerical error and lowest computational and human costs. Adaptive mesh refinement is one of such techniques, and is developed to find such a solution by dynamically refining and coarsening meshes until a desired accuracy is achieved. The number of computational points is thus adapted to the asked accuracy and human effort is limited as the procedure is designed to be automatic. For complex flow solvers, the focus remains on the adaptation of mesh without making major changes in the code and thus employing such a refinement technique is of significant value here. The two key elements of any adaptive method are the error estimation and the mesh adaptation technique. The most important part an adaptive procedure is the development of such error detection method which could indicate the regions where the mesh adaptation should be performed.

The choice of adequate refinement criteria for minimizing the analysis errors is of special interest for adaptive mesh refinement. In adaptive mesh refinement, the cell refinement is carried out in the regions of significant flow activity. Major features like shocks, boundary layers and shear layers, vortex flows, mach stems, expansion fans and the like exist in various flows and a fine mesh is required to capture such regions with accuracy. Each feature has some physical characteristics which can serve as a tool for the adaptive grid refinement because such parameters can indicate the regions of flow activity. These sensing parameters are known as error indicators and are becoming an effective tool for adaptive mesh refinement.

The present study is a part of the effort to build several error indicators or refinement criteria for the automatic mesh adaptation method developed for ISIS-CFD, the unstructured volume-of-fluid finite volume RANSE flow solver developed at Ecole Centrale de Nantes. The grid refinement method is flexible so that new refinement criteria and can easily be added to the code. In this study, three refinement criteria based on the absolute value of gradients of the field variables, i.e. pressure and velocity, and vorticity are analyzed for the automatic grid refinement.

Chapter 2 presents the refinement methodology implemented in ISIS-CFD. The steps of the automatic grid refinement are also discussed. Chapter 3 deals with the refinement criteria used in this study. A simple vortex flow problem is set to study different aspects of the refinement criteria and to examine their behavior for automatic grid adaptation. Chapter 4 and 5 deal with two test cases employed to judge the performance of the refinement criteria in more detail. These sections describe the efficiency of the refinement criteria in different conditions.

2 Adaptive grid refinement in ISIS-CFD

In this introductory chapter, mesh adaptation procedure in ISIS-CFD is described. It is based strongly on the work of A. Hay [2] and Wackers and Visonneau [3].

2.1 The flow solver ISIS-CFD

The **ISIS-CFD** flow solver, available as a part of the FINE^{TM}/Marine computing suite, uses the incompressible unsteady Reynolds-averaged Navier Stokes equations (RANSE). The solver is based on the finite volume method to build the spatial discretization of the transport equations [1]. The face-based method is generalized to two-dimensional, rotationally-symmetric, or three-dimensional unstructured meshes for which non-overlapping control volumes are bounded by an arbitrary number of constitutive faces. The velocity field is obtained from the momentum conservation equations and the pressure field is extracted from the mass conservation constraint, or continuity equation, transformed into a pressure-equation. In the case of turbulent flows, additional transport equations for modeled variables are solved in a form similar to the momentum equations and they can be discretized and solved using the same principles. Incompressible and non-miscible flow phases are modeled through the use of conservation equations for each volume fraction of phase. The whole discretization is fully implicit in space and time and is formally second order accurate. Several near-wall low-Reynolds number turbulence models, ranging from one-equation Spalart–Allmaras model, two-equation k–ω closures, to a full Reynolds stress transport Rij –ω model are implemented in the code.

2.2 Mesh adaptation

The partial differential equations that govern fluid flow and heat transfer are not usually amenable to analytical solutions, except for very simple cases. Therefore, in order to analyze fluid flows, flow domains are split into smaller sub domains (made up of geometric primitives like hexahedra in 3D and quadrilaterals and triangles in 2D). The governing equations are then discretized and solved inside each of these sub domains. Typically, one of three methods is used to solve the approximate version of the system of equations: finite volumes, finite elements, or finite differences. ISIS-CFD is based upon the finite volume discretization. Care must be taken to ensure proper continuity of solution across the common interfaces between two sub domains, so that the approximate solutions inside various portions can be put together to give a complete picture of fluid flow in the entire domain. The sub domains are often called elements or cells, and the collection of all elements or cells is called a mesh or grid.

Mesh adaptation refers to the modification of an existing mesh so as to accurately capture flow features. Generally, the goal of these modifications is to improve resolution of flow features without excessive increase in computational effort. ISIS-CFD employs the h-refinement methodology also known as **Mesh adaptation method** [2]. As generally viscous flow in complex geometries and unstructured meshes are dealt, p-refinement is difficult to apply because the unstructured meshes do not lend themselves to the development of numerical schemes of higher orders. In addition, the solutions being addressed may not be smooth (Multi-fluid flows) and in this case r-refinement necessarily lead to non-orthogonal grids, which is not useful for the proper treatment of viscous terms. That is why their use is limited to almost non-viscous flow (Euler equations). Moreover, these methodologies sometimes have lack of generality, especially in the case of complex geometries in three dimensions. Adaptive mesh methods can be further divided into two categories:

- **Adaptive mesh generation**: This type of method employs successively the use of computer code and mesh generation software. After a first run of the solver on an original grid, it determines the size *h* of local mesh necessary anywhere in the field of calculation to ensure accuracy desired. This information is exploited by the mesh to generate an adapted grid to be used for another simulation. Both steps are repeated until the final expected solution is reached.

- **Dynamic local mesh adaptation**: This method is employed in ISIS-CFD solver. As part of these methods, the mesh is adapted directly in the computer code. Again, it performs a first simulation from an initial grid and the result obtained makes it possible to determine which changes must be brought to the local *h* size for the desired precision. A certain number of operations are then applied to the grid. Once these modifications are undertaken inside the solver, simulation is run again. These two stages are repeated until final solution is obtained. This category of methods can be further divided into two types by distinguishing methodologies from superimposed grids and those of single grids. When superimposed grids are considered, patches of refinement are superimposed on the initial grid and a procedure is developed to couple the basic patches and grid between them. This principle gave rise to the AMR (Adaptive Mesh Refinement) method which remains one of best known methods. In the single grid methods, the whole of the adapted grid is treated in a single way like in the case of uniform grids, which requires the use of not-structured grids.

Looking in more detail the differences between these two types of methodology, main advantages of the methods of local automatic adaptation of mesh as compared to those of adaptive mesh generation are the following:

- **Absence of input/output**: The adaptation of mesh is made directly in the computer code, it does not require entering and exiting at each step in software.

These various inputs/outputs are computing time consuming and require many operations. Thus, the lack of input/output gives an advantage in terms of computing time. This benefit is more important as the number of stages of refinement/de-refinement increases. In addition, whole methodology requires only one software.

- **Dynamic Adaptation**: The second advantage of the strategy is somewhat linked to the previous one. Since the adaptive process is an integral part of ISIS-CFD, connectivity of the adapted grids will be accomplished in a dynamic way. Again, the number of calculation for the creation of connectivity will be decreased as well and most importantly, we are able to know and to retain the kinship links between the cells of the mesh. This allows us to make the rapid adjustments since part of the mesh can simply be reversed to previous state. In addition, we have the opportunity to get the original mesh.

- **Minimizing user intervention**: During an adaptive calculation, the user uses one software only. Compared to a mono-grid calculation, only few additional parameters are to be specified. Thus, the adaptation of grid can be carried out without requiring any new intervention of the user. That thus makes it possible to reduce human costs of computations.

- **Parallel Computing**: For three-dimensional complex applications, it is necessary to use parallel machines to reduce the computing time and access to large memory available. Again, it is preferable to have maximum integration. While it is necessary to leave the solver and rebuild the entire mesh, this is very disadvantageous for the effectiveness of parallel simulations in case of adaptive mesh generation.

2.3 Local mesh adaptation in ISIS-CFD

2.3.1 Organization and data structure

This section shows how the data is organized within the code in order to achieve the mesh adaptation. This organization of data is important for several reasons. At first, it will determine the capacity of the adaptive process in terms of versatility and adaptability. Thus, the organization of data makes it possible to achieve all the changes you want to perform on the mesh. Secondly, the organization of the data will influence the computing time of the code as well as that of the grid adaptation. Finally, the data structure will determine the ease of programming in the computer code. All these elements indicate that the data must be organized and dealt with care. To store the refined grids, the normal ISIS-CFD data structure is used. This data structure contains the locations of the nodes and connectivity pointers between cells, faces, and nodes.

For refinement, only a few extra pointers are added. These include an indicator of the basic type of each cell (hexahedron etc.) and pointers to indicate those faces that form one divided face.

2.3.1.1 Relationship between the cells

The concept of relationship or family ties between members of the same category of cells leads to a data structure tree. The concept of kinship between members of the same category is important to address several problems at once. At first, it allows to easily perform de-refinement which will be detailed later. Secondly, we are able to get the initial mesh. This means that after a number of stages of refinement/de-refinement, an area of the computational domain can (if necessary) become identical to its initial configuration. Lastly, and in the third time, relationship between the cells will make it possible to carry out a very fast dynamic adaptation. Indeed, when elements to be adapted have a relationship (upstream or downstream), the modifications to be carried out is simply the activation or deactivation of the members of this relationship.
Note that this does not limit the generality of adaptation since it does into account the way the cells are refined or de-refined.

There is a family tree data structure used here. At one stage of refinement, one cell divided into several smaller cells will be seen as a mother cell with a number of daughter cells who are sisters among themselves thus resulting in a family. If these daughters are later refined they will become mothers and naturally there common mother will become grandmother. Therefore during the adaptation process, kinship will grow or shrink in a dynamic way. When one speaks about a family, one refers to the family ties between two successive generations. Thus, a family of cells corresponds to a mother and her daughters but not to the grandmother or to the possible grand-daughters. Thus, a cell can belong to several families either as a mother, or as a daughter.

Mother-daughter-sister (MDS) connectivity associates three numbers with each cell. The first corresponds to the number of its mother cell, the second with the number of one of daughters and the third with the number of one of these sisters. Thus, the way in which the cells are divided or grouped, each cell has always only three explicit bonds of relationship. And, these daughters are pointed between themselves with the family ties of the sister type. Thus, to identify all the daughters of a mother, it is enough to point the first daughter then looping over her sisters until again falling down on the first daughter of the family. That is illustrated on figure 2.1. The advantage this type of storage is that the number of integers associated with each cell is fixed and it requires less memory locations than storing all the daughter cells of a mother cell. Note that a cell wire always has a single mother and at least a sister.

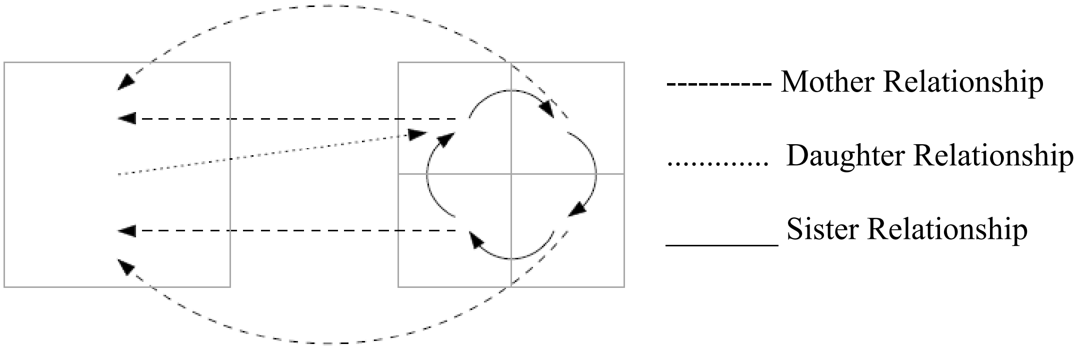
---------- Mother Relationship
.... Daughter Relationship
________ Sister Relationship

Figure 2.1: Mother-daughter-sister connections between cells of the same generation.

On several generations, the family ties between the cells accumulate naturally and give rise to a data structure tree as illustrated on figure 2.2.

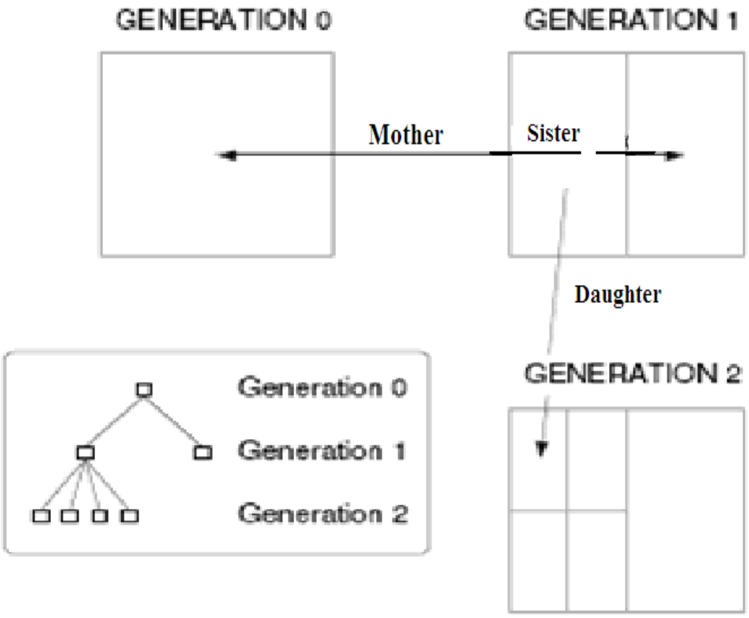

Figure 2.2: Mother-sister-daughter connections of cells between several generations.

2.3.1.2 Activity of the cells

This concept makes it possible to determine the use of a cell during computation on the current grid. It provides local adaptive method with the choice to manage multiple grid generations at the same time. The cells of different meshes coexist in the data structures of computer code. It is thus necessary identify the state of activity of a cell. Three states can be distinguished:

- **Active cells:** active cells correspond to the cells which play a part on grid being used for the current computation. These cells are integral parts of the grid being processed. In particular, active control volumes are those on which the discretization of the equations is carried out.

- **Dead cells:** dead cells correspond to the useless cells with regard to the grid currently being used. They are preserved in the data structure as to be possibly re-used in some other adaptation stage for example de-refinement. The dead cells have neither faces nor a state vector but only the information about its family ties is stored.

- **Destroyed cells**: These are the dead cells which are not preserved in the data structures of the computer code. These cells must disappear completely from the tables allowing memory to be used for other active or dead cells.

2.3.2 Grid refinement and coarsening

The choices for refinement are important with regard to the adaptive procedure since it will guarantee its effectiveness and generality. De-refinement of the cells is also concerned with the choices selected but only in an indirect way. Indeed, de-refinement of the cells is simply to undo any earlier refinement.

To decrease the size of an element of the grid, it is enough to divide it into smaller cells. For each type of volume, there exist many possibilities of divisions. Division of an element is always done by preserving the topology of the cells. Thus, the division of a quadrangle leads to the generation of smaller quadrangles, division of hexahedron results in generation of smaller hexahedra, Figure 2.3, and so on. Also, division of the cells should not lead to highly stretched and bad quality cells.

Current refined meshes consist of hexahedra cell types but other geometrical cell types like but prisms, pyramids, and tetrahedra can be added easily. ISIS-CFD has face-based discretization so the faces of these cells can be divided into smaller faces. Thus, cells can be refined into smaller cells, while their neighbour cells remain the same. Such type of divided faces can also be present in original grids as now a day, commercial mesh generators like HEXPRESS^{TM} of FINE^{TM} /Marine can creates such type of meshes.

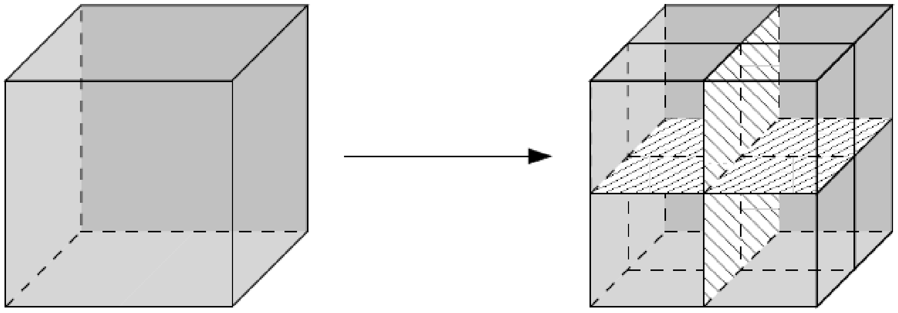

Figure 2.3: Isotropic refinement of a hexahedron.

Sometimes the need for directional refinement is also stressed e.g. for sheared flows (wake, boundary layer, jet, etc). The main point of directional refinement is the way in which one will select the direction of refinement. Again, the topology of the cells must be preserved. Possible directional refinements are represented in figures 2.4 for the quadrangles.

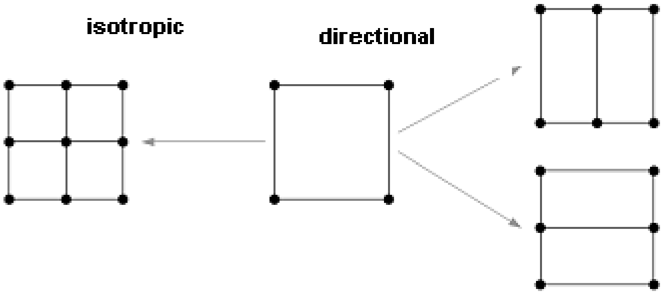

Figure 2.4: Refinements of a quadrangle.

Finally, a non-refined neighbor of a refined cell presents a so called hanging node which is accounted for naturally by our face-based FV method: a face with a hanging node is simply seen as several smaller faces. A 2D case of hanging node is shown in figure 2.5

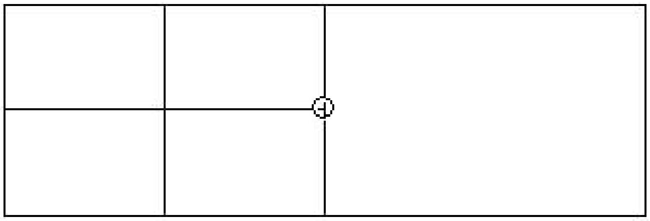

Figure 2.5: Hanging node.

The main goal of an adaptive procedure is to achieve a desired accuracy of the solution and reduce the errors without putting any extra effort. As the mesh can possibly be too fine in some region for the desired accuracy, it can be coarsened by an agglomeration strategy. The coarsening of mesh areas which are previously refined is simple and can be accomplished by reversing the process of refinement.

2.3.3 Refinement procedure

The stages of the refinement method in ISIS-CFD are described now. In general the method works as follows: the flow solver is run on the initial grid for a limited number of time steps. Then the refinement process is called to adapt the grid. The refinement procedure has a specific refinement criterion, if the criterion, based on the current solution indicates that certain parts of the grids are not fine enough and needs to be refined, the grid is refined and the solution of on the initial grid is copied to the new refined grid. The flow solver is run again and the refinement procedure is called and the refinement criteria decide what changes are to be made to the grid i.e. to refine or de-refine the grid. The process is repeated until the convergence is obtained for the steady flows and grid is no longer changed if the refinement procedure is called again as illustrated in figure 2.6.

In order to make the process more flexible the refinement procedure can be divided into three distinct parts. Each part can be dealt separately as these parts exchange minimal information between them [3]. The parts are:

1) Refinement criterion: the refinement criterion or error indicator is an essential part of the adaptive process. The refinement criterion decides which parts of the grids are to be refined or de-refined based on a certain threshold value. Various refinement criteria can be developed based on gradients or curvature information of the flow variables such as pressure, temperature or velocity or other error estimators. A distinction of the refinement criteria can also be based on the scalar or vector like the state variables. The important point is that an error indicator can be developed which may not depend on the type and orientation of the cells and thus avoiding the need for developing separate refinement criterion for different cell types. These error indicators are the main part of the current study and will be discussed in detail in the next chapter.

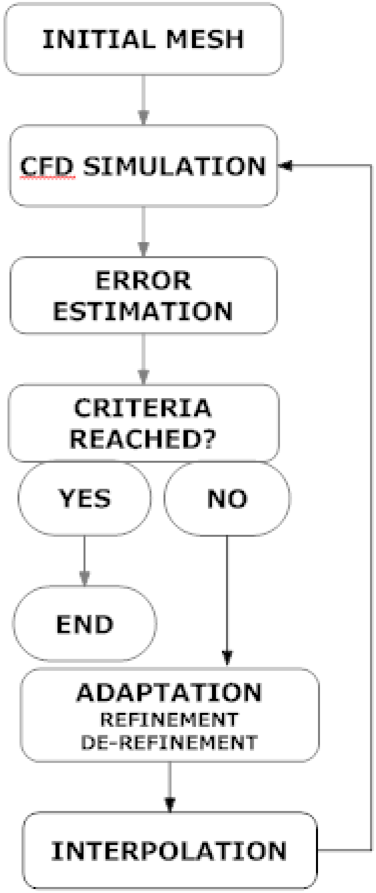

Figure 2.6: Adaptive procedure.

2) Refinement decision: next step is the refinement decision based upon the refinement criterion in which a list of flags is created indicating which cell will be refined and in case of directional refinement, the direction is also specified. This decision depends upon the cell type but not on the way the refinement criterion was computed. It is simply an evaluation of the criterion field. The refinement decision has two steps. First, the refinement criterion is evaluated in each cell, based on a certain threshold value the refinement decision is taken. If the value of the refinement criteria exceeds the threshold value, the cell is refined and if it is below the threshold the cell will be de-refined. Similar methodology applies to the directional refinement, if the refinement criterion exceeds the threshold in a certain direction, the cell will be refined in that direction and vice versa. In the second step the decision in each cell is adapted to its neighbor cell. Certain quality criteria are required in order to produce good solutions: a face of a cell should not be divided more than two times which would result in too large difference between the cell and its neighbors and secondly, the angle between the cell centre/face centre line should not be too large which will decrease the quality of faces' reconstruction. Keeping that in view, refining a cell may require the refinement of its neighbor cells or may prevent these neighbor cells from being de-refined. As a result, in an iterative procedure, refinement decisions are added and de-refinement decisions are removed. Completion of the refinement decisions is a great advantage before the start of the refinement. For example, it is much convenient to remove a de-refinement decision than to undo an already completed de-refinement.

3) Refinement: The final step is the actual refinement of the grid. First, all cells selected for de-refinement are de-refined, and then refinement of all cells to be refined is performed. During refinement, new small size cells are created, faces and nodes are added between them, and the cell family ties are adjusted; for de-refinement, small size cells are merged into their original large cells, unnecessary faces are removed, and the original family ties are restored. In parallel, once the refinement decisions are taken, the grid in each block can be refined without any communication with the other blocks. Both refinement and de-refinement are done cell by cell to ensure maximum generality and robustness of the code. After the treatment of each single cell, a correct grid with all its pointers is left, even if some pointers have to be changed again later when a neighbor cell is refined. In this way, a cell to be refined can treat all its faces and neighbors the same manner, no distinction is needed between cells that are already refined, cells that still have to be refined, and cells that are not refined at all. To further increase the generality of the code, the parts that refine cells and faces are completely decoupled.

3 Error indicators for adaptive mesh refinement

The use of grid adaptation allows having more accurate solutions with limited number of grid points. One of concerns for adaptive grid refinement is selection of adequate refinement criteria for minimizing analysis errors. In adaptive mesh refinement, the selection of "parent cells" to be divided is made on the basis of regions where there is appreciable flow activity. It is well known that in various flows, the major features would include shocks, boundary layers and shear layers, vortex flows, mach stems, expansion fans and the like. It can also be seen that each feature has some "physical signature" that can be numerically exploited. For example, shocks always involve a density/pressure jump and can be detected by their gradients, whereas boundary layers are always associated with rotationality and hence can be detected using the curl of velocity [7]. In compressible flows, the velocity divergence, which is a measure of compressibility, is also a good choice for shocks and expansions. These sensing parameters which can indicate regions of flow where there is activity are referred to as **error indicators** and are very popular in adaptive mesh refinement for CFD.

Control of the refinement and/or coarsening via the error indicators or refinement criteria can be undertaken using various parameters as refinement criteria. These are conventionally based on the gradient or curvature information of flow variables such as pressure, temperature or velocity. More sophisticated parameters can be lift, drag or momentum etc. in addition to that the refinement criterion can be a scalar or vector field like the state variables. As indicated above every flow has some typical physical signatures which can be exploited and used as an error indicator. For example in two-phase flows the refinement criterion can be refinement around the free-surface based on the volume fraction value in the cells. The important thing is, that the criterion in a cell may not depend on the cell type, or on its orientation. This makes it easy to change criteria, as it is never necessary to develop a separate criterion for each cell type. For different refinement criteria, this part is the only one that changes. The object of the current study is to build various refinement criteria for the flow solver ISIS-CFD. This effort is a part of the plan to develop a series of different refinement criteria so that the user of the solver could choose the criterion best suited to his problem.

The velocity, pressure and vorticity are important parameters for describing a particular flow. Therefore it is very natural for refinement criteria to be based upon such variables. So we define error indicators using gradients of pressure and velocity, and vorticity value. The indicator value is represented by the Euclidian norm of the gradients in three dimensions in case of pressure and velocity. In case of vorticity the indicator value is based on the Euclidian norm of vorticity.

3.1 Refinement Criteria

Pressure gradient criterion

In this criterion the error indicator value is based on the norm of the pressure gradient which can be described for 3D as:

$$||\nabla_p|| = \sqrt{(\frac{\partial p}{\partial x})^2 + (\frac{\partial p}{\partial y})^2 + (\frac{\partial p}{\partial z})^2}$$

Velocity gradient criterion

Similarly the norm of the velocity gradient can be described as:

$$||\nabla_v|| = \sqrt{(\frac{\partial u}{\partial x})^2 + (\frac{\partial u}{\partial y})^2 + (\frac{\partial u}{\partial z})^2 + (\frac{\partial v}{\partial x})^2 + (\frac{\partial v}{\partial y})^2 + (\frac{\partial v}{\partial z})^2 + (\frac{\partial w}{\partial x})^2 + (\frac{\partial w}{\partial y})^2 + (\frac{\partial w}{\partial z})^2}$$

Vorticity criterion

The norm of the vorticity is defined as:

$$||\omega|| = \sqrt{\omega_x^2 + \omega_y^2 + \omega_z^2}$$

Where

$$\omega_x = \frac{\partial w}{\partial y} - \frac{\partial y}{\partial z}$$

$$\omega_y = \frac{\partial u}{\partial z} - \frac{\partial w}{\partial x}$$

$$\omega_z = \frac{\partial v}{\partial x} - \frac{\partial u}{\partial y}$$

Based on the indicator value we can set a threshold value on which refinement and de-refinement take place. This threshold can be described as:

Threshold value = max (cell size × refinement criterion value)

During refinement process if the product of cell size and refinement criterion value becomes greater than the provided threshold, refinement will take place and vice versa.

We can also control the refinement procedure by indicating the number of generations. Refining for one generation means that the cell will be refined one time during the refinement procedure. If we opt for more number of generations the cell and the daughter cells will go on being refined that much time until the threshold value is reached. So in this way by adjusting the threshold value and the number of generations, the mesh refinement can be performed with desired accuracy and low computational cost.

3.2 A simple vortex flow problem

The refinement criteria described above can now be tested and compared in order to determine their ability and efficiency to control automatic grid refinement. There are many flows in which the production of vortices occurs. Applications are the bilge vortex of a ship that hits the propeller plane, the tip vortices of an aircraft wing (that can cause problems for following aircraft), and vorticity shed by cars.

A trailing vortex has a high-velocity core; on an unrefined grid the velocity in this core is reduced by numerical errors, so that the computation predicts the wrong vortex strength. Refinement criteria can be used to indicate the position of a vortex core. The goal is to show that we can accurately compute the position and the strength of a vortex using refined grids and compare various refinement criteria in order to choose the best one.

We consider a simple vortex flow in a cylinder, the flow is introduced at one end of the cylinder and the vortex strength is analyzed at various cross sections, for our analysis we consider the cross-sections near to the exit of the cylinder to observe the strength of the vortex and see the performance of various error indicators. Along the lines, we also compare the uniform refinement and the automatic refinement as well.

The geometry is shown below and the prescribed boundary conditions at the inlet and outlet are Dirichlet and zero pressure gradient respectively.

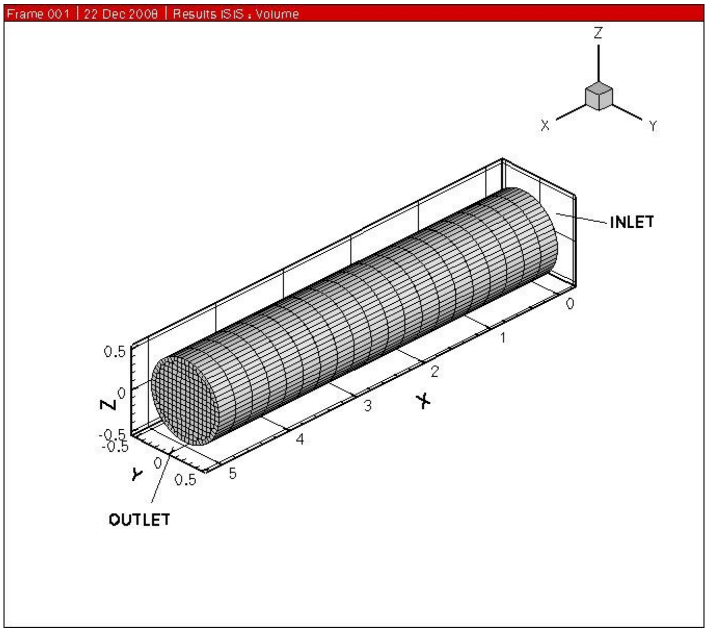

Figure 3.1: Cylinder geometry and computational domain.

We are interested in studying the effect of refinement criteria in reducing the discretization error. As vortex flow problems have a singularity in the centre of the vortex and are not smooth, it is difficult to estimate the error and instead the pressure integral value at a surface can be an alternate in analyzing the performance of a refinement criterion because the pressure integral goes to minus infinity for the exact solution, so for the numerical solutions, lower pressure integral value will correspond to better performance. So we calculate the pressure integral value at a cross section close to the outlet of the cylinder at x = 4.5m. We start with flow computations on the uniform grids first; four grids ranging from coarse to very fine are used and the pressure integral is computed at the cross section near the outlet. The results are given in the table 3.1.

No of cells	**Pressure Integral at X-section x= 4.5**
4.4×10^3	-7.58×10^{-1}
3.4×10^4	-8.9×10^{-1}
2.7×10^5	-1.06
2.1×10^6	-1.132

Table 3.1: Uniform grids data.

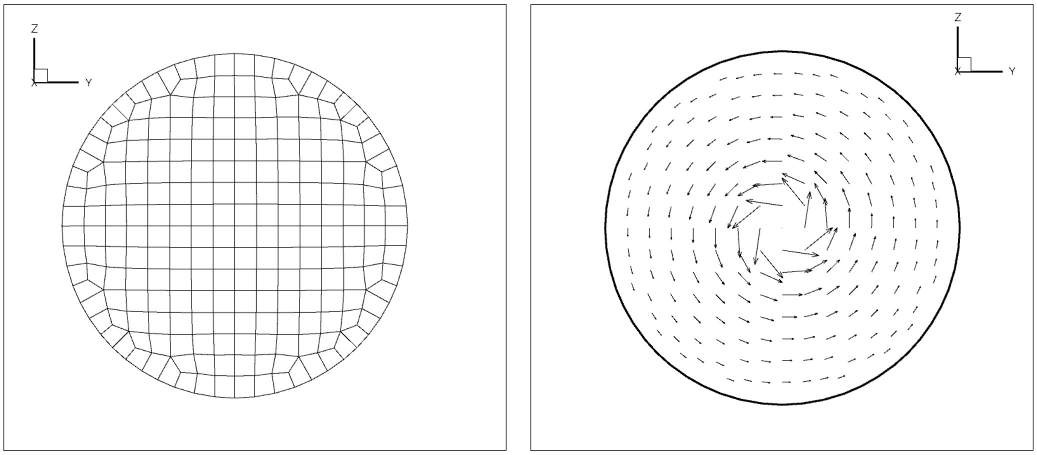

Figure 3.2:The coarse 4.4K cell Uniform grid cross section (left) with vortex on the right.

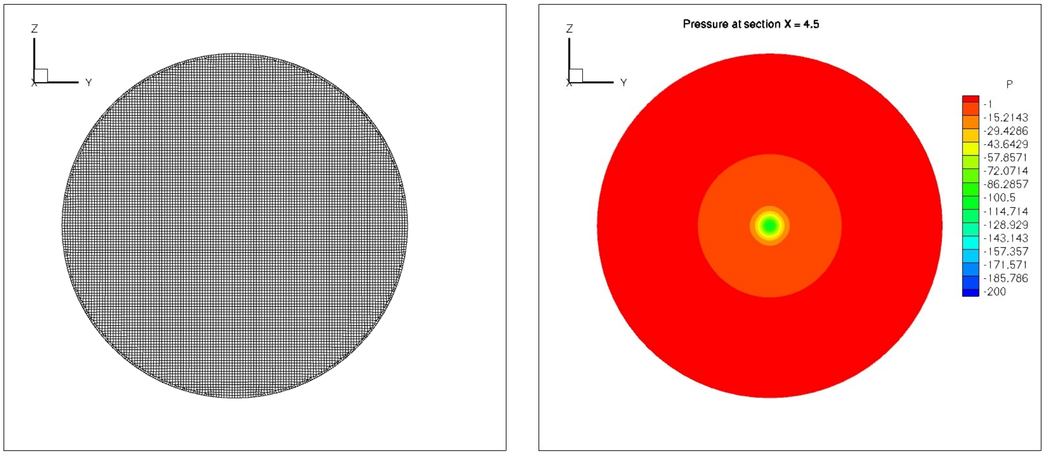

Figure 3.3: The refined 2.1M cells uniform grid and pressure contour at X-section x=4.5.

The next step is to go for adaptive grid refinement using the three refinement criteria. We take an initial grid having 4.4×10^3 cells and perform adaptive grid refinement controlled by threshold values and the number of generations. Threshold values are determined by the number of cells which should be initially marked for refinement or de-refinement. Higher the number of cells chosen for refinement, more refined the grid will be and vice versa. In this way, for a particular criterion, we try different threshold values and eventually select one which will give that desired number of cells marked for refinement/de-refinement. In order to compare refinement criteria, the threshold values are set so that number of cells initially selected to be refined/de-refined are equal for each criteria. In this way we can compare which criterion gives the minimum number of cells after to reach a particular pressure integral value. The data is tabulated and plotted in the tables 3.2 to 3.4.

Threshold value	**No of generations**	**No of cells**	**Pressure Integral**
0.1	1	1.5×10^4	-8.70×10^{-1}
	2	5×10^4	-9.85×10^{-1}
	3	1.7×10^5	-1.11
	4	5.77×10^5	-1.194
0.3	1	1×10^4	-8.71×10^{-1}
	2	2.6×10^4	-9.54×10^{-1}
	3	7.6×10^4	-1.08
	4	2.5×10^5	-1.165
0.4	1	9.2×10^3	-8.72×10^{-1}
	2	2.3×10^4	-9.56×10^{-1}
	3	6.5×10^4	-1.08
	4	2×10^5	-1.54
0.7	1	7.4×10^3	-9.1×10^{-1}
	2	1.6×10^4	-9.94×10^{-1}
	3	4.3×10^4	-1.10
	4	1.3×10^5	-1.19

Table 3.2: Automatic grid refinement data for velocity gradient criterion.

Threshold value	**No of generations**	**No of cells**	**Pressure Integral**
0.3	1	1×10^4	-8.54×10^{-1}
	2	1.9×10^4	-9.70×10^{-1}
	3	4.3×10^4	-1.114
	4	1.2×10^5	-1.135
0.4	1	8.5×10^3	-8.58×10^{-1}
	2	1.9×10^4	-9.62×10^{-1}
	3	4.1×10^4	-1.11
	4	1×10^5	-1.2
0.5	1	8×10^3	-8.18×10^{-1}
	2	1.8×10^4	-9.65×10^{-1}
	3	3.8×10^4	-1.15
	4	1×10^5	-1.19
0.9	1	7.4×10^3	-9.43×10^{-1}
	2	1.3×10^4	-9.72×10^{-1}
	3	3.3×10^4	-1.132
	4	8.6×10^4	-1.24

Table 3.3: Automatic grid refinement data for vorticity criterion.

Threshold value	**No of generations**	**No of cells**	**Pressure Integral**
18	1	1×10^4	-8.61×10^{-1}
	2	3×10^4	-9.44×10^{-1}
	3	1×10^5	-1.06
	4	4×10^5	-1.14
45	1	8.8×10^3	-8.66×10^{-1}
	2	2.2×10^4	-9.7×10^{-1}
	3	6.4×10^4	-1.092
	4	2.4×10^5	-1.145
53	1	8.3×10^3	-8.68×10^{-1}
	2	2.1×10^4	-9.67×10^{-1}
	3	6×10^4	-1.09
	4	2.3×10^5	-1.19
64	1	7.9×10^3	-8.57×10^{-1}
	2	1.9×10^4	-9.84×10^{-1}
	3	5.9×10^4	-1.11
	4	2×10^5	-1.20

Table 3.4: Automatic grid refinement data for pressure gradient criterion.

The data given in the tables above is plotted in figures 3.4 to 3.6. We note that all the three criteria are capturing the flow features and identify the zones for refinement. The criteria also respond to the threshold values correctly i.e. increasing the threshold value decreases the number of cells to be refined. The mesh refinement using the criteria also results in much lower number of cells than that of uniform refinement for a given pressure integral value. Figures 3.8 and 3.9 show the adapted grids for various grid generations. All the criteria are able to produce smooth refinement.

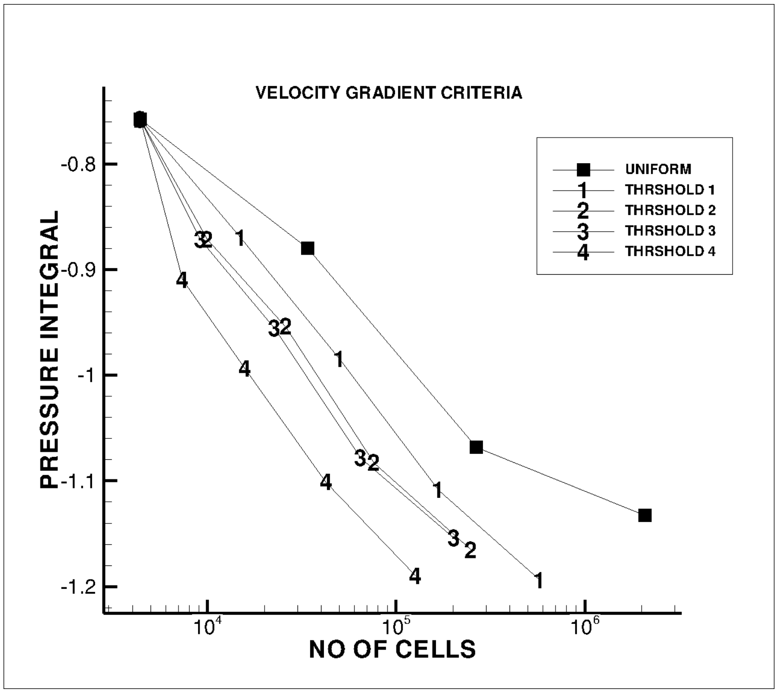

Figure 3.4: Pressure integral plot for velocity gradient criterion at x = 4.5.

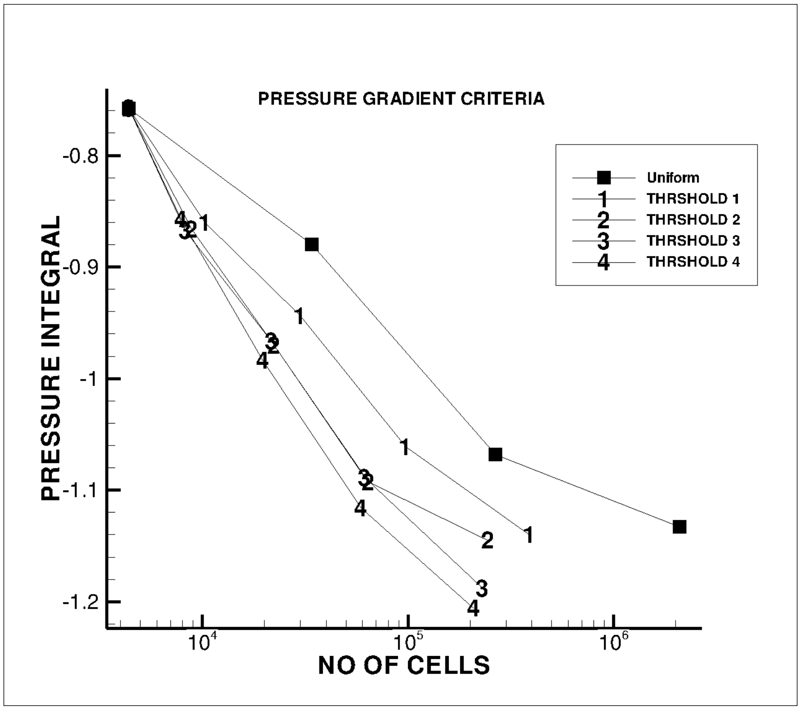

Figure 3.5: Pressure integral plot for pressure gradient criterion at x = 4.5.

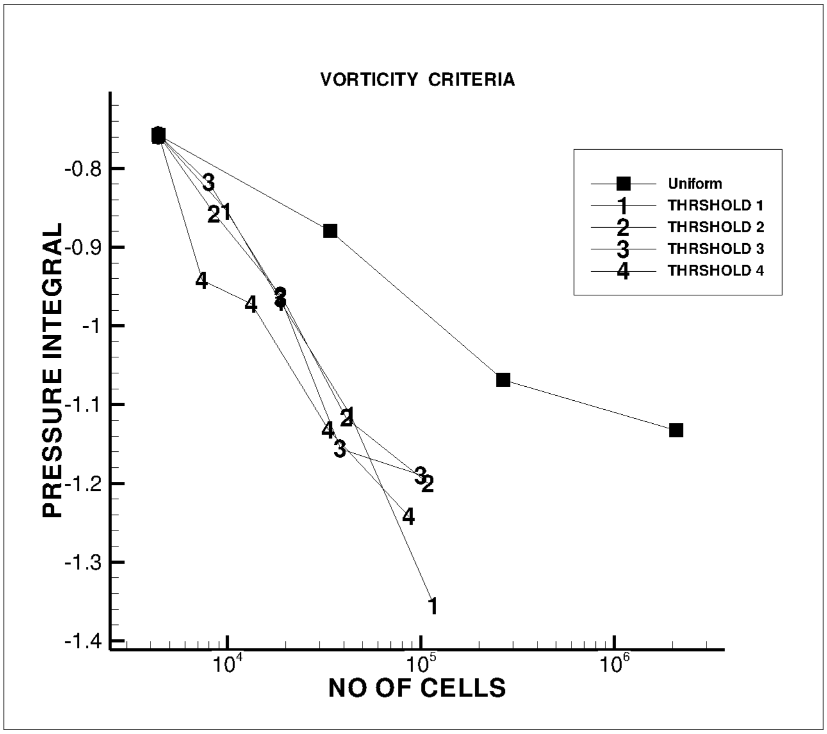

Figure 3.6: Pressure integral plot for vorticity criterion at x = 4.5.

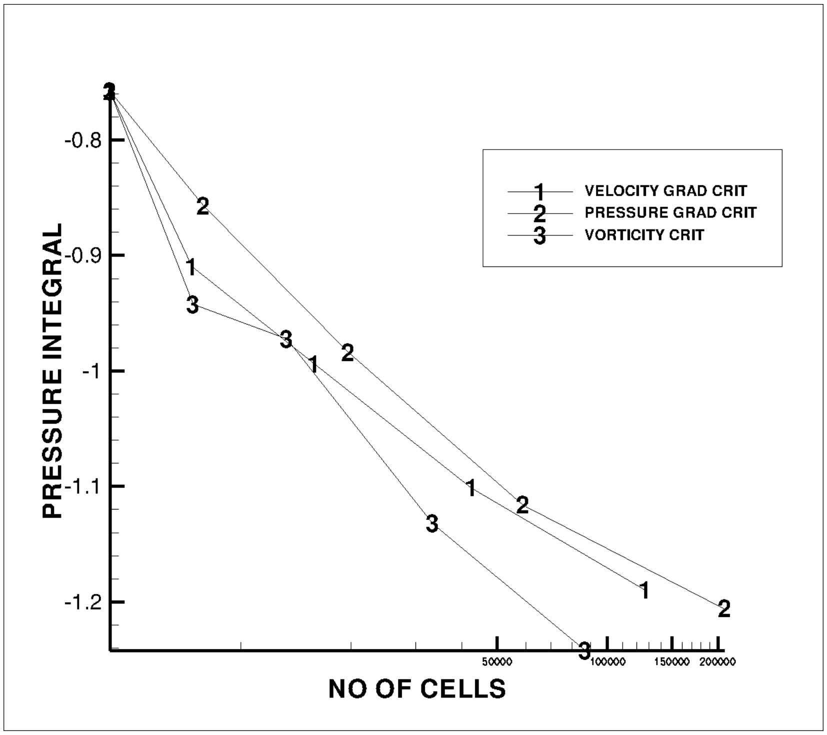

Figure 3.7: Pressure integral plot for three criteria at x = 4.5 for maximum threshold.

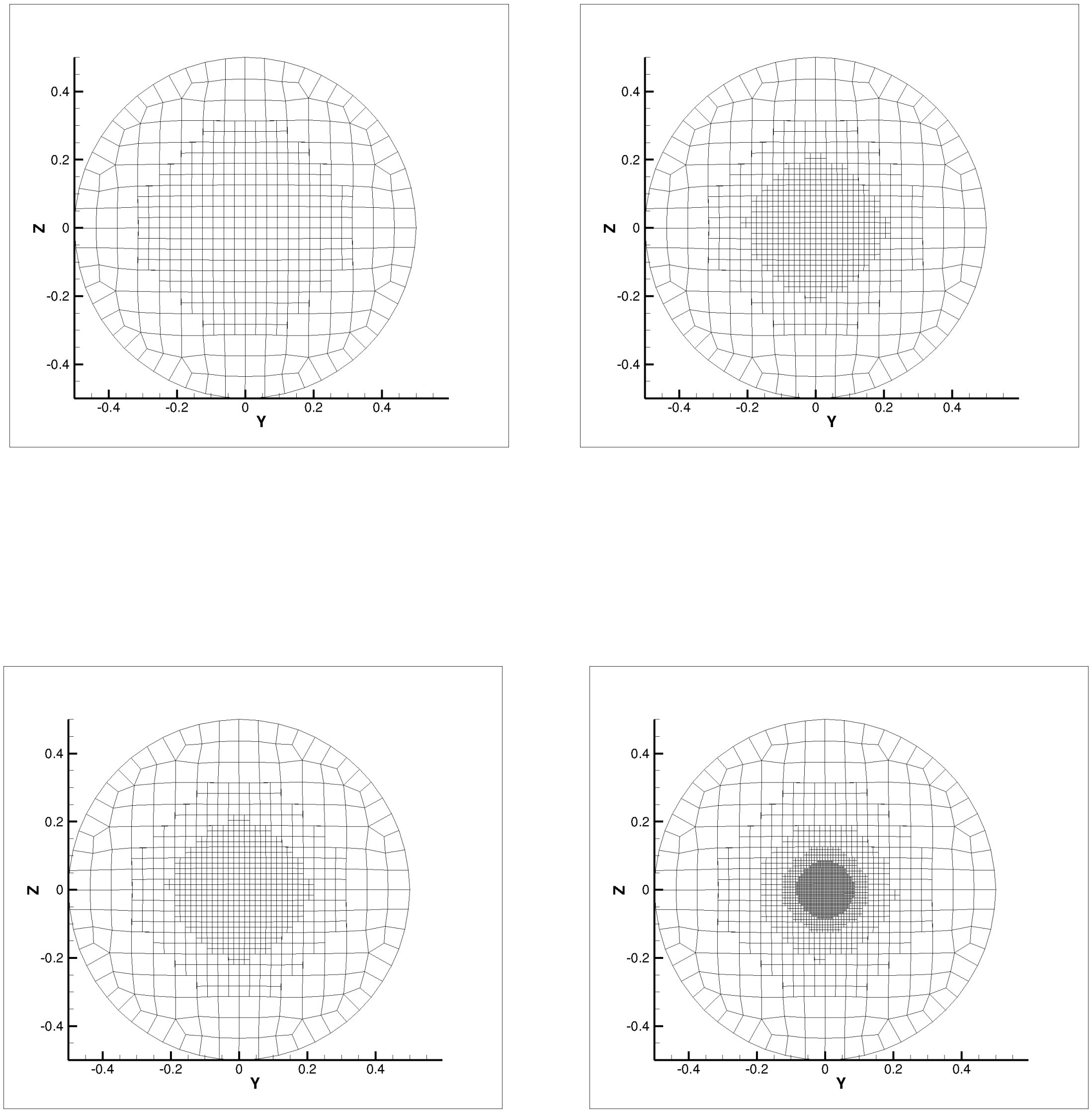

Figure 3.8: Effect of number of generations on the refinement for velocity gradient criteria.

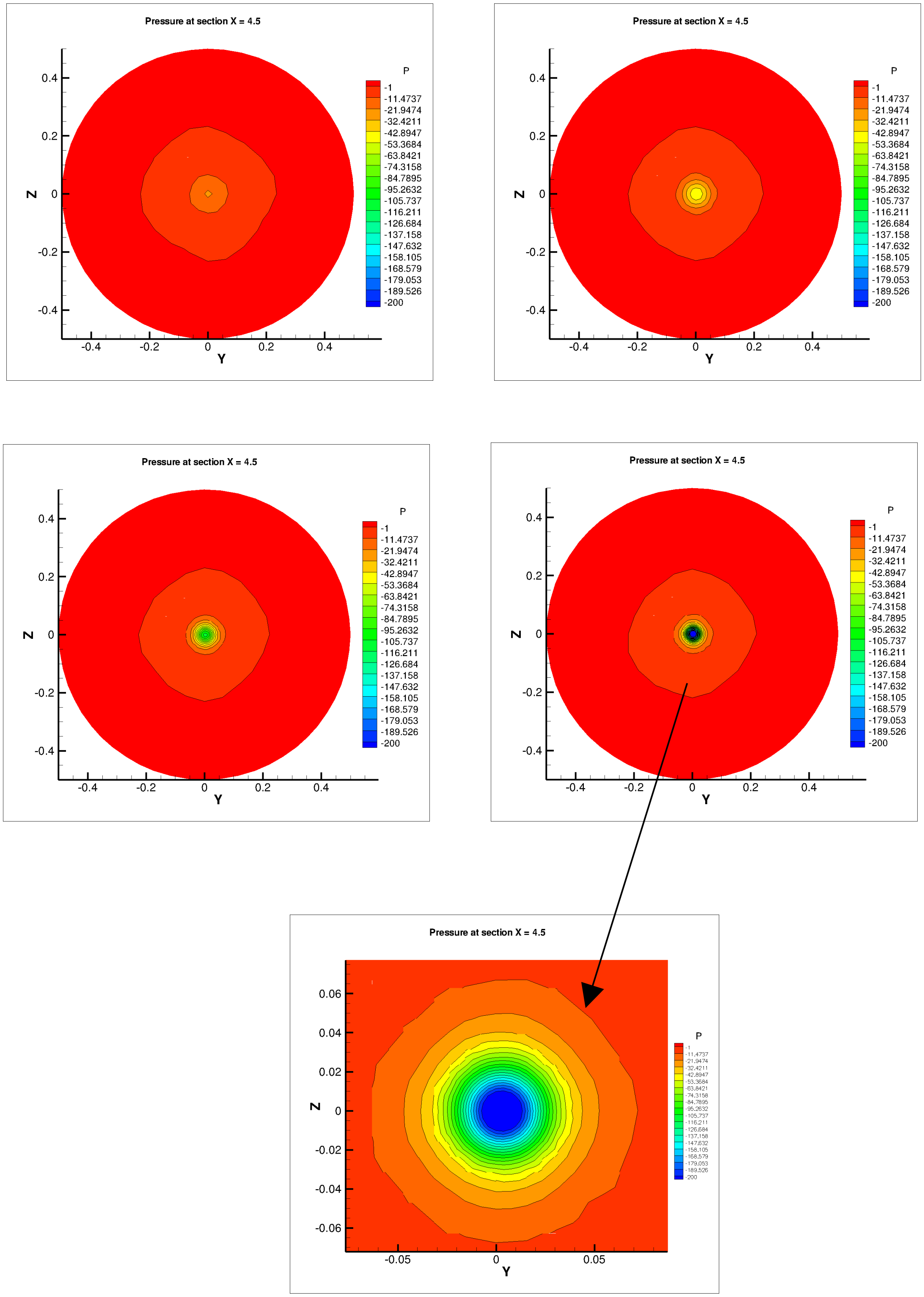

Figure 3.9: Pressure contours for velocity gradient criterion at maximum threshold for four generations.

4 KVLCC2 Test Case

In the previous chapter we analyzed the behavior of various refinement criteria for a simple vortex flow in a cylinder and established that all the criteria were identifying the refinement areas and capturing vortices by varying degree of accuracy. Now we analyze these error indicators with more complex test cases. The aim is to check these criteria in different conditions such as varying turbulence models and effect of the boundary layer refinement.

As the focus in this project is on the capturing of vortices we analyze the bilge vortices behind a ship in this section and check the ability of the criteria to predict such vortices accurately. Traditionally, the interest in the wake flows has been focused on the so-called "hooks" in the propeller plane which are zones of low axial velocity. The presence of strong vorticity is responsible for the creation of such hooks.

For this purpose the KVLCC2 test case is chosen. This test case has been extensively analyzed in the past and a very detailed data are now available and secondly the hooks discussed above are particularly present as shown by the experimental data. So predicting such hooks along with the other flow features with the refinement criteria is of particular importance in this section.

4.1 Geometry and conditions

The original hull form KVLCC2 was conceived by Korean Institute of Ships and Ocean Engineering (KRISO) to provide data for both explication of flow physics and CFD validation for a modern tanker ship with bulbous bow. The main features of the ship at model scale level are given below [4]:

Length between perpendiculars	L_{PP}	= 5.5172 m
Breadth	B / L_{PP}	= 0.1813
Draft	d / L_{PP}	= 0.0650
Wetted surface area,	S_0 / L_{PP}^2	= 0.2656
Block coefficient	C_b	= 0.8098
Reynolds number	Re	= 4.6×10^6

Figure 4.1: KVLCC2 scale model.

4.2 Computations

Computations are started from a very coarse mesh, to see if the refinement criterion is able to effectively create an entire fine mesh. The initial grid has 60 K cells. The three criteria use three threshold values and three number of generation for each threshold. The third criteria is restricted to two generation only due to high computational cost and CPU time in case of three no of generations. The initial computations are performed using the k-ω SST turbulence model. We can choose, in ISIS-CFD, whether to perform boundary layer refinement or not. If we opt for boundary layer refinement, cells in the boundary layers in the directions normal to the wall will be refined only. Here the boundary layer refinement is also carried out. The threshold values and the grid size data is presented in the tables 4.1, 4.2 and 4.3.

Threshold value	No of generations	No of cells after refinement
4.35	1	9.8×10^4
	2	1×10^5
	3	1×10^5
3.5	1	1.3×10^5
	2	1.4×10^5
	3	1.4×10^5
4.4×10^{-1}	1	1.9×10^5
	2	6.3×10^5

Table 4.1: Automatic grid refinement data for velocity gradient criterion

Threshold value	No of generations	No of cells after refinement
4.35	1	9.8×10^4
	2	1×10^5
	3	1×10^5
3.5	1	1.3×10^5
	2	1.4×10^5
	3	1.4×10^5
4.4×10^{-1}	1	1.8×10^5
	2	6.2×10^5

Table 4.2: Automatic grid refinement data for vorticity criterion

Threshold value	No of generations	No of cells after refinement
8.2	1	1.1×10^5
	2	2.3×10^5
	3	4.5×10^5
18	1	1.6×10^5
	2	4.1×10^5
	3	9.7×10^5
35	1	2.2×10^5
	2	8×10^5

Table 4.3: Automatic grid refinement data for pressure gradient criterion

4.3 Results

4.3.1. Effect of the boundary layer refinement

Meshes and velocity field contours at the propeller plane are given in figures 4.2 to 4.10. Plots are for the three refinement criteria with different threshold and no of generations. If we look at the refined mesh of first two thresholds in case of velocity gradient and vorticity criteria we see that there is no significant refinement in the propeller plane as compared to initial mesh. The pressure gradient criterion performs better than the other two. The main reason behind this phenomenon is that the velocity gradients and the vorticity are high in the boundary layer region. If we go for boundary layer refinement the two criteria respond to this zone which results in the unnecessary and costly refinement in the boundary layer and little refinement in the other regions. On the other hand, the pressure gradient criterion avoids such refinement in the boundary layer because the pressure varies little in that zone. The boundary layer is only refined there, where it is dictated by the outside flow. This is the main advantage of the pressure gradient criteria over the other two and results in more accurate flow features predictions.

The boundary layer refinement effect is also depicted in the refined grid size resulting form various number of generations. A kind of saturation phenomenon occurs here. As shown in the tables 4.1, 4.2 and 4.3, we see that for the velocity gradient and vorticity criteria, the first two thresholds have very little increase in the grid size going from one number of generations to three. So for higher threshold values, the number of generations becomes insignificant. The pressure gradient criterion does not follow such trend and there is a significant increase in the number of cells if we increase the number of generations for a particular threshold value. The threshold value being very low in case of third threshold, allows the velocity gradient and vorticity criteria to refine the zones out of the boundary layer as well.

Limiting streamlines are also shown in the figures for various refinement criteria and conditions. All criteria, generally, follow the same pattern: the upper lines move backwards all the way onto the upper part of the stern. The lines start to move downward at about mid girth and become more vertical approaching the stern. Near the bilge the lines moving downward meet the lines from bottom and here a vortex type separation occurs and the created vortex sheet rolls up into the bilge vortex.

Among the three criteria, the hook shape in the propeller plane is best captured by the pressure gradient criteria due to the reasons explained above. As the turbulence model used here is k-ω SST, later in the section it will be shown that the EASM turbulence model performs even better than the k-ω SST model and accurately captures the hook shape.

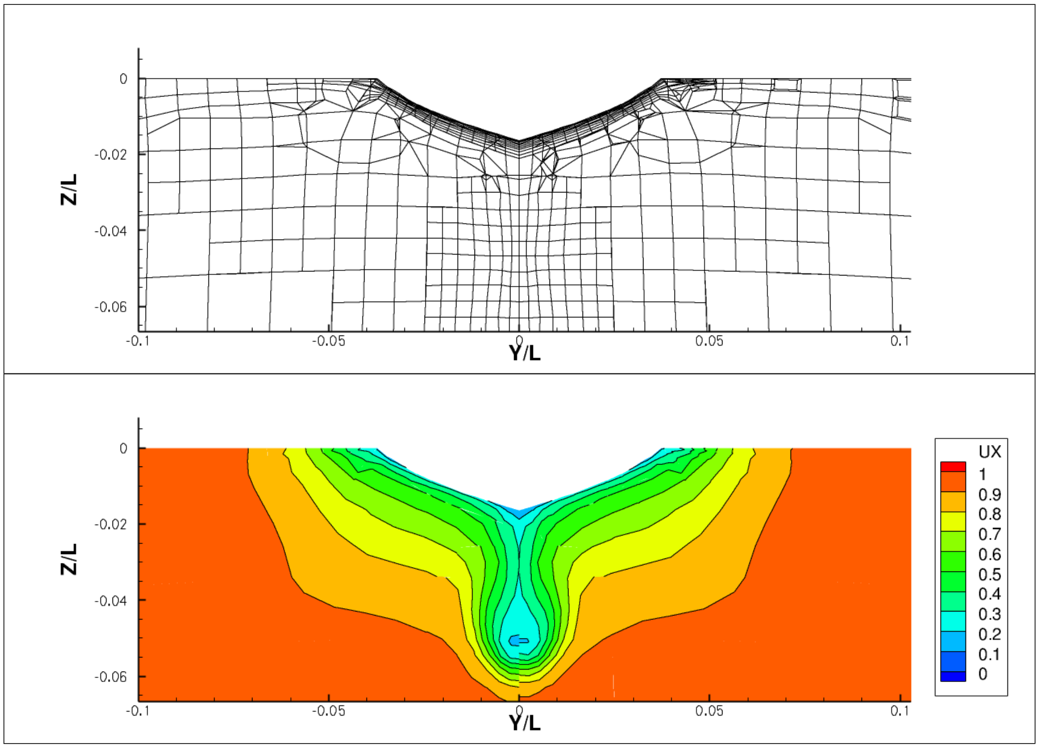

Figure 4.2: Velocity gradient criterion for 1st threshold and 3 generations. Propeller plane Mesh and axial velocity contour. Original mesh is on left and refined mesh on right.

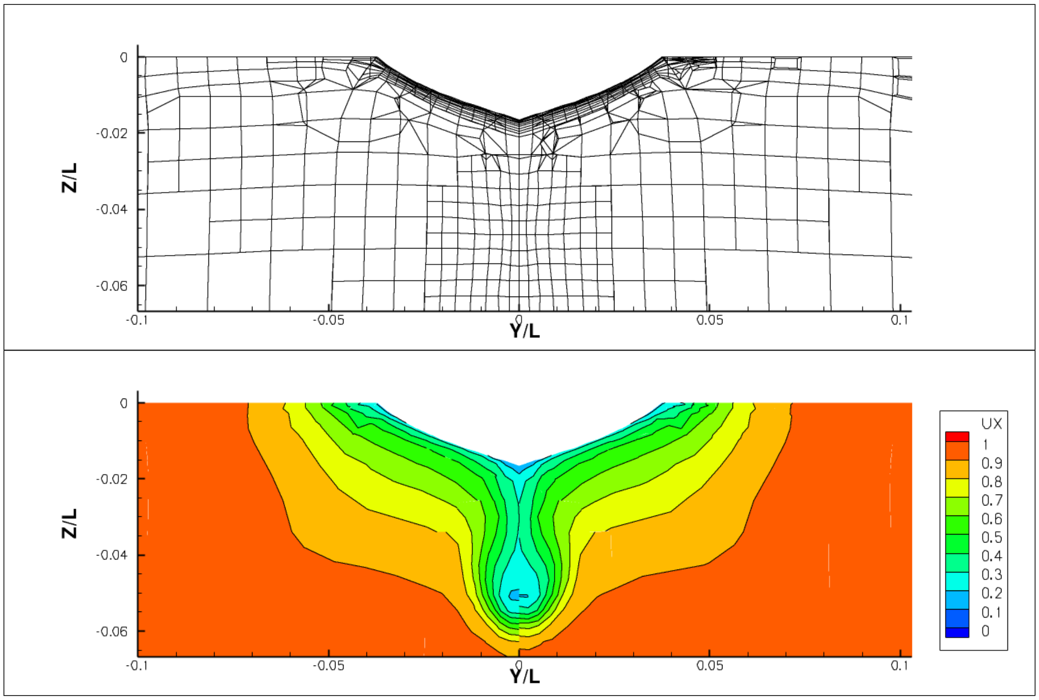

Figure 4.3: Velocity gradient criterion for 2nd threshold and 3 generations. Propeller plane Mesh and axial velocity contour. Original mesh is on left and refined mesh on right.

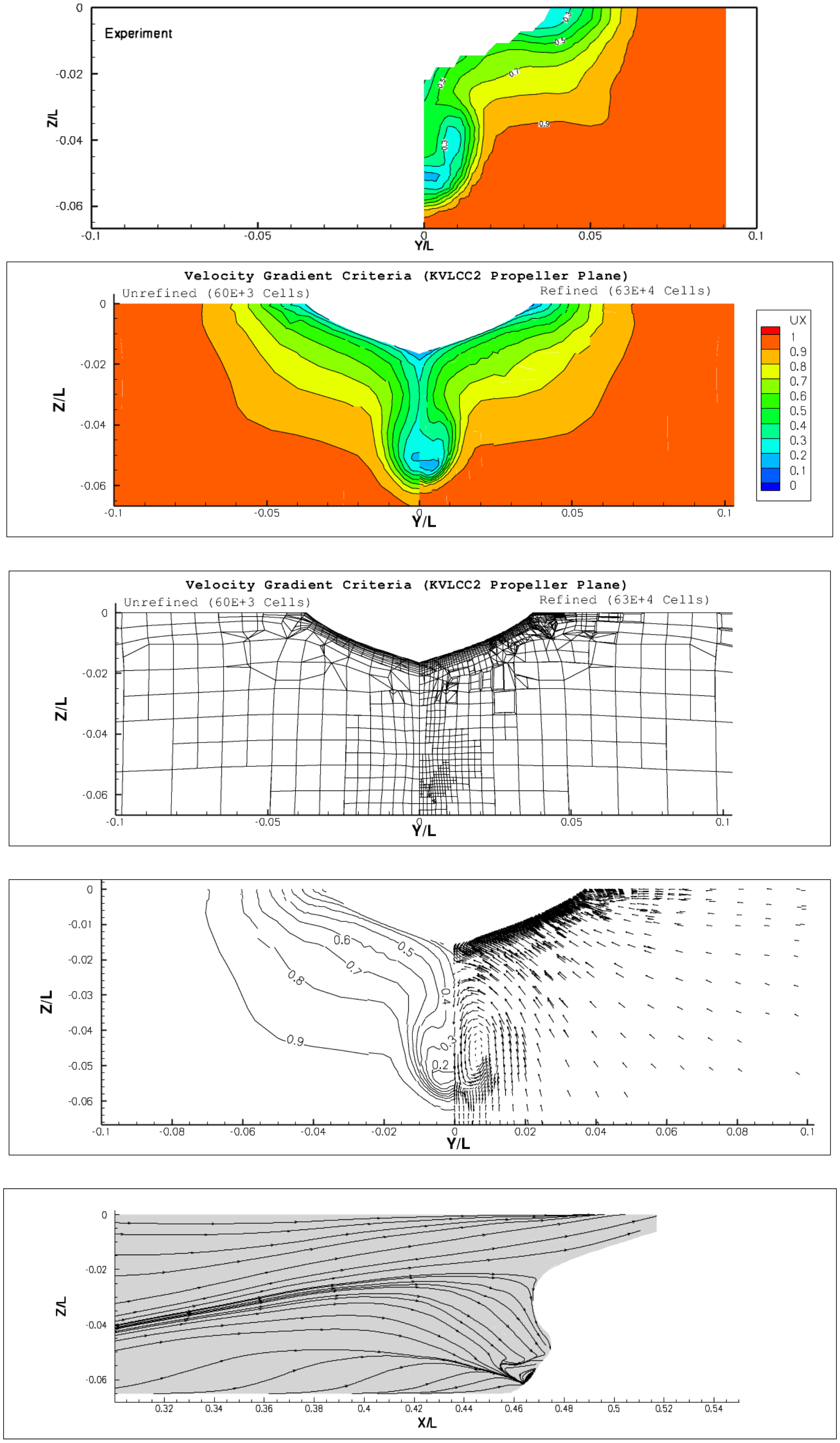

Figure 4.4: Velocity gradient criterion for 3rd threshold and 2 generations. Propeller plane Mesh, axial velocity contour, cross flow vectors and streamlines.

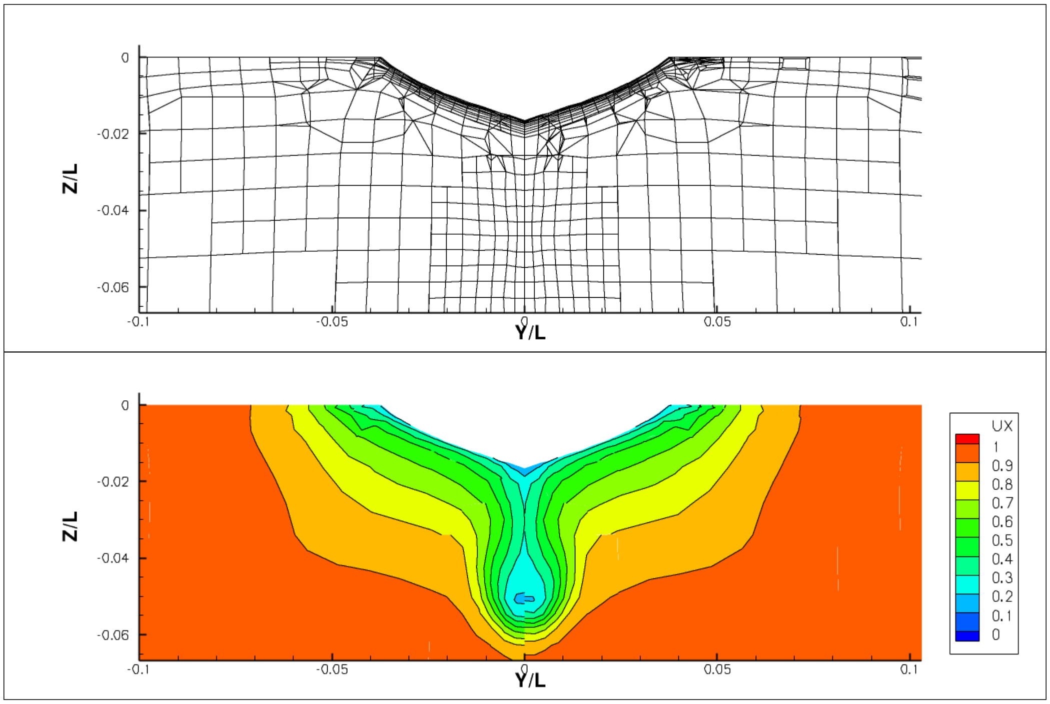

Figure 4.5: Vorticity criterion for 1st threshold and 3 generations. Propeller plane Mesh and axial velocity contour. Original mesh is on left and refined mesh on right.

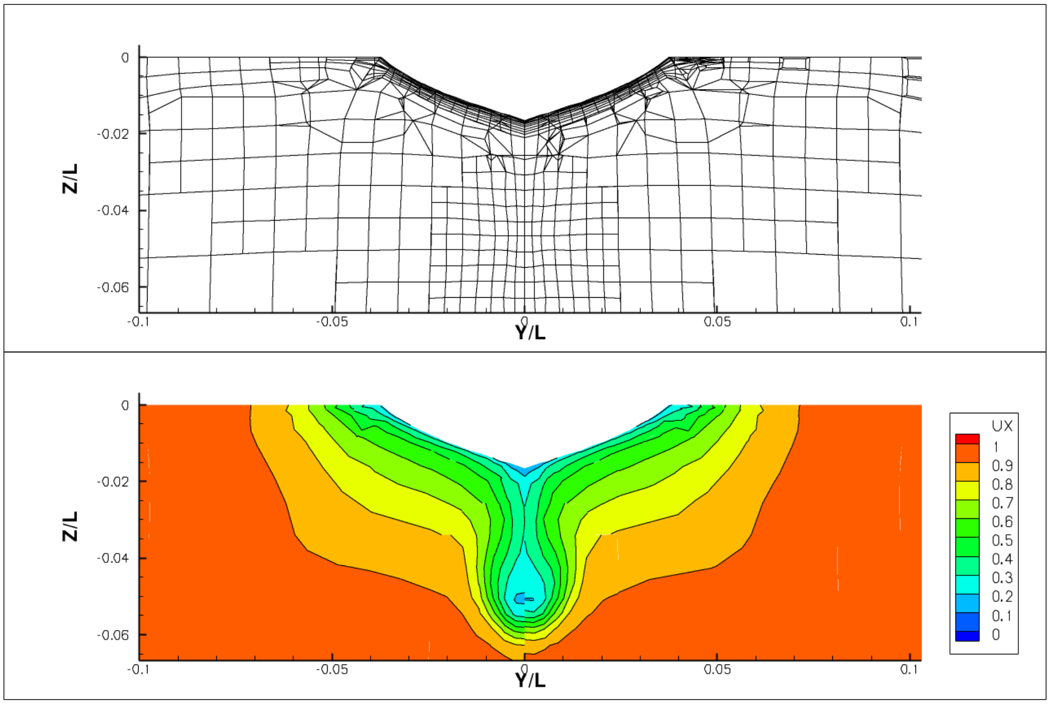

Figure 4.6: Vorticity criterion for 2nd threshold and 3 generations. Propeller plane Mesh and axial velocity contour. Original mesh is on left and refined mesh on right.

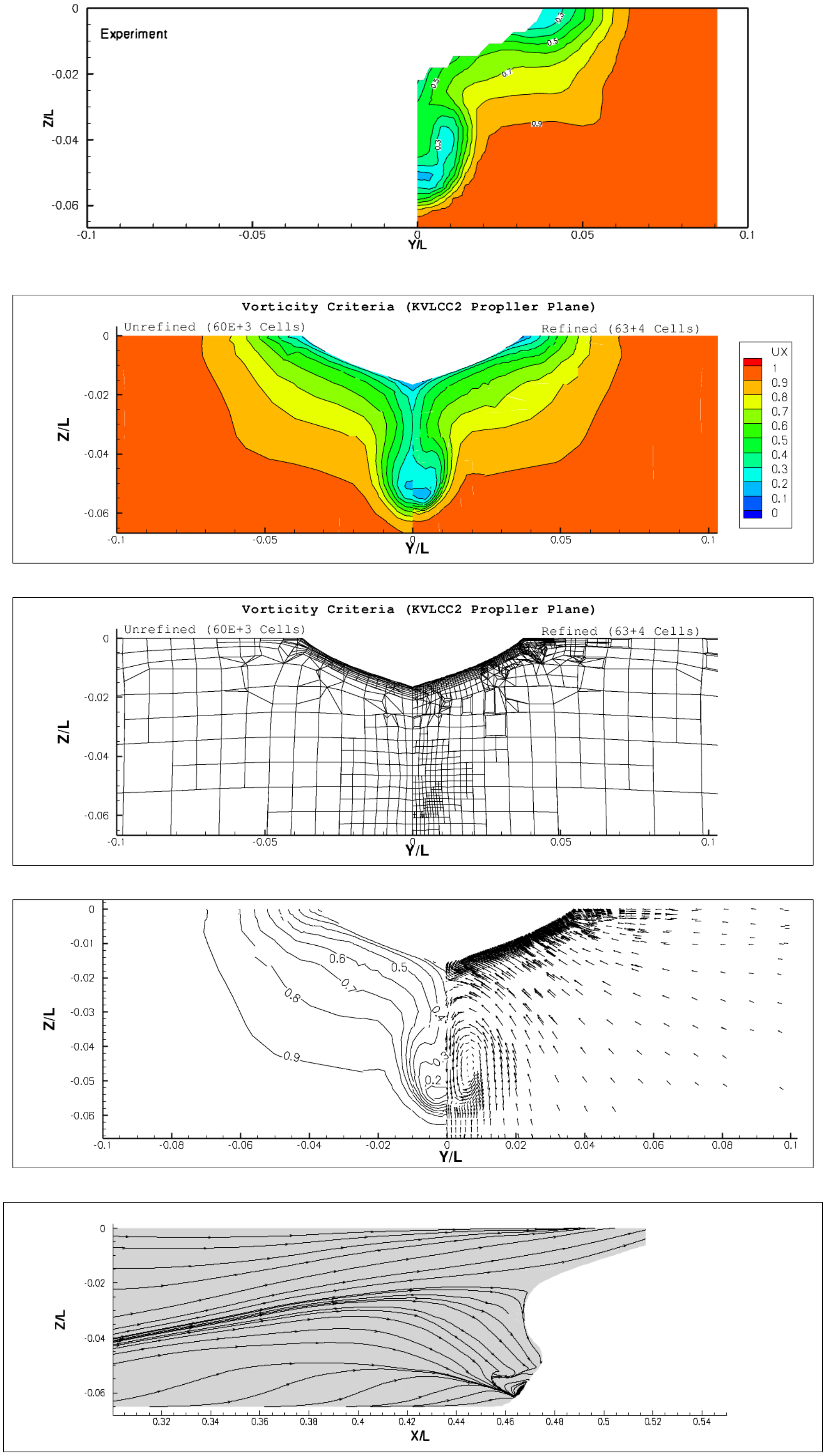

Figure 4.7: Vorticity criterion for 3rd threshold and 2 generations. Propeller plane Mesh, axial velocity contour, cross flow vectors and streamlines.

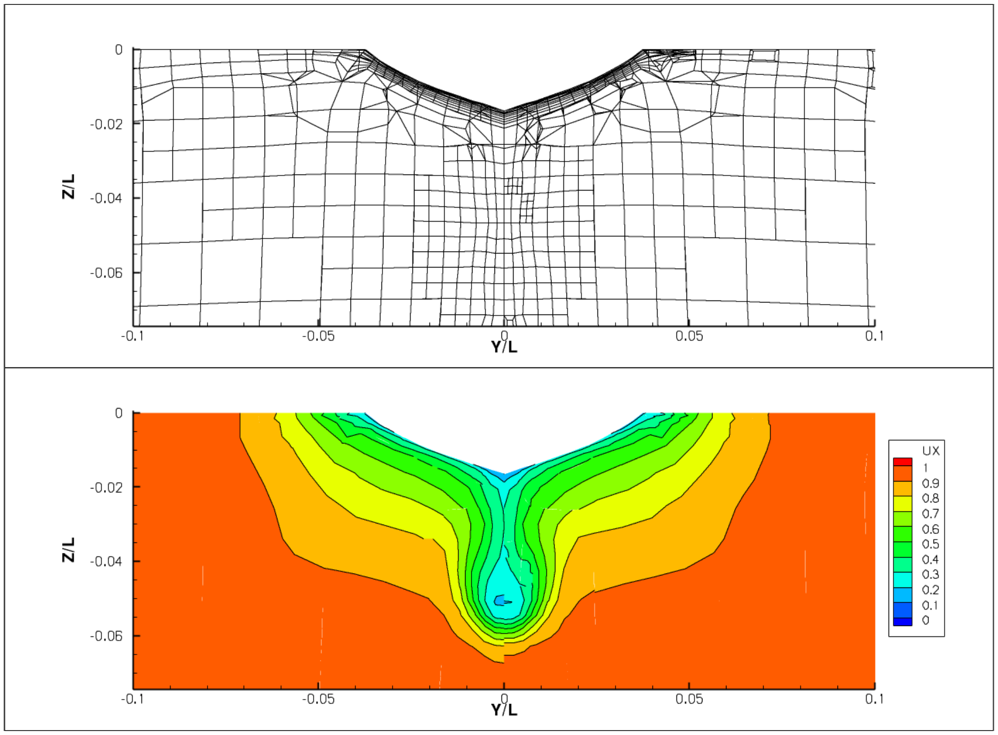

Figure 4.8: Pressure gradient criterion for 1st threshold and 3 generations. Propeller plane Mesh and axial velocity contour. Original mesh is on left and refined mesh on right.

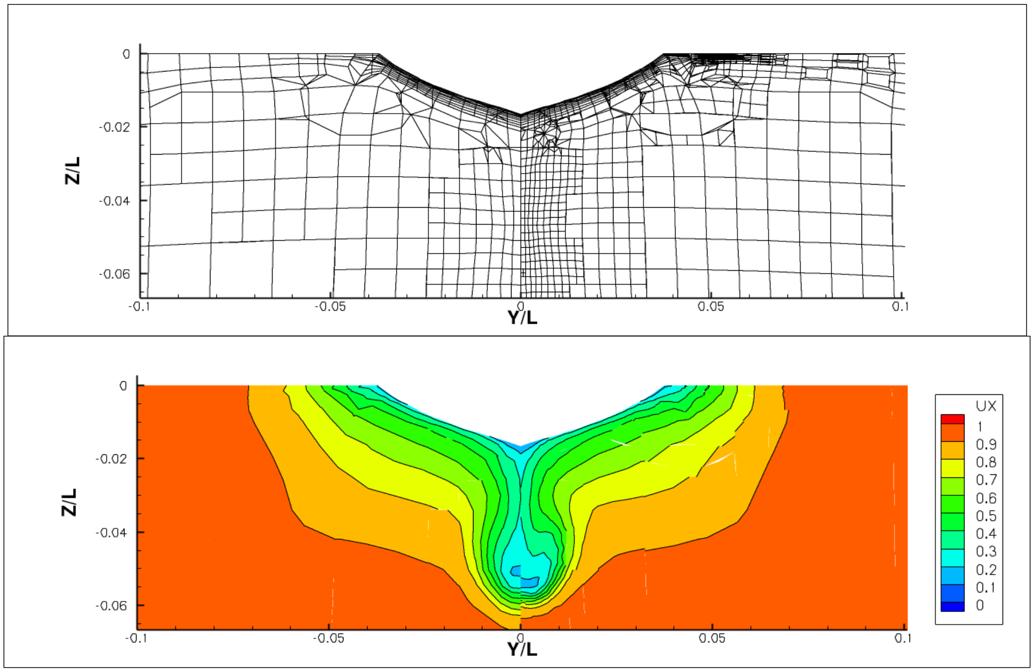

Figure 4.9: Pressure gradient criterion for 2nd threshold and 3 generations. Propeller plane Mesh and axial velocity contour. Original mesh is on left and refined mesh on right.

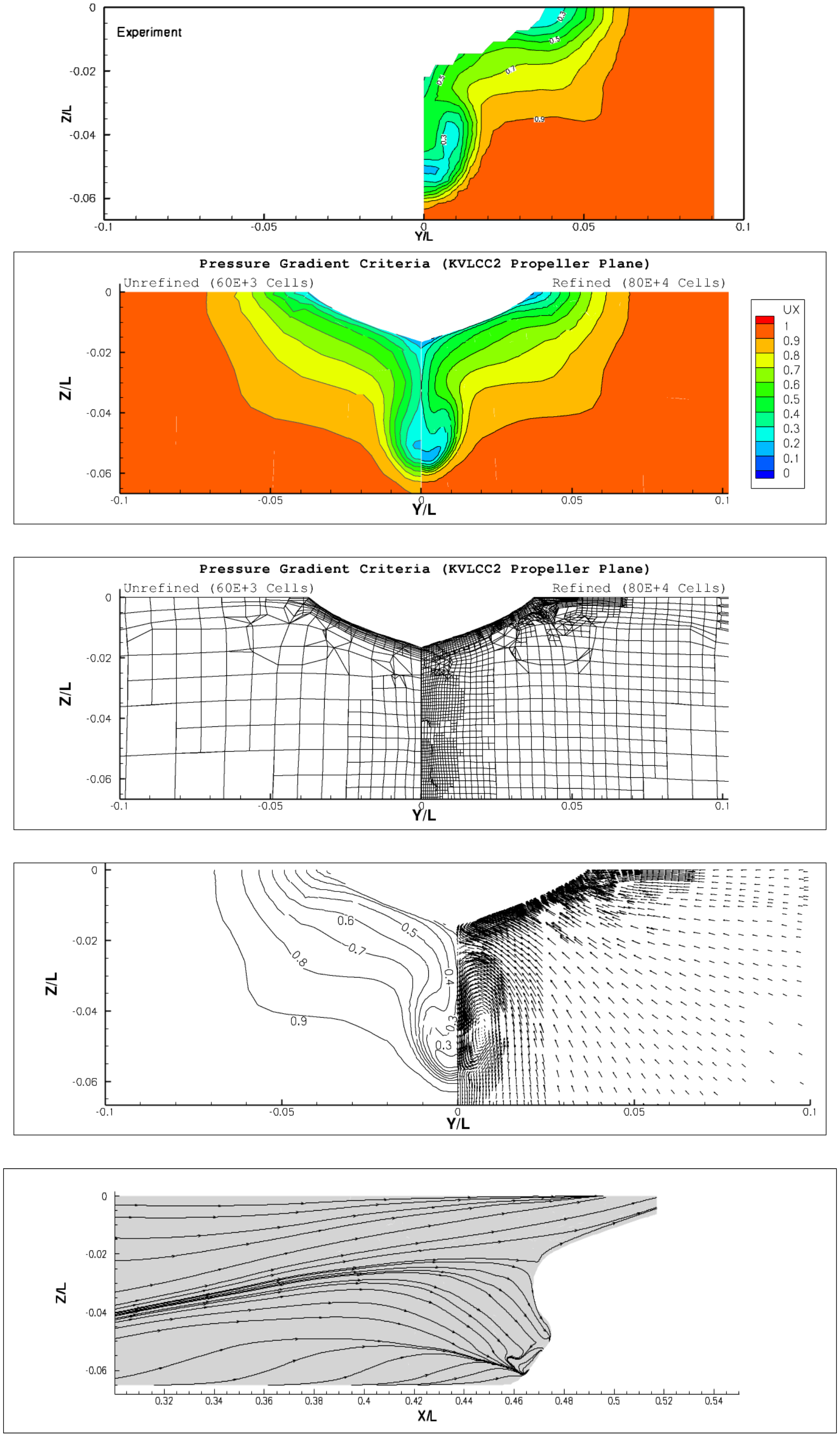

Figure 4.10: Pressure gradient criterion for 3rd threshold and 2 generations. Propeller plane Mesh, axial velocity contour, cross flow vectors and streamlines.

4.3.2 Computations without boundary layer refinement

As we noted in the last section that boundary layer refinement caused the velocity gradient and vorticity criteria to behave improperly, a few computations are performed without boundary layer refinement and the results improve for the two criteria. The computational data is presented in table 4.4 and the plots are given in figure 4.11 to 4.13. We note that velocity gradient and velocity criteria are responding to the flow features outside the boundary layer. Changes in the number of generations also significantly effect the refined grid size. The pressure criterion is behaving as expected and flow is still better especially in the region around Y=0.05, Z=-0.04 and is also preferred due to its generality.

Refinement criteria	Threshold value	No of generations	Cells after refinement
Velocity gradient	7×10^{-2}	1	2.1×10^5
		2	7.7×10^5
Vorticity	3×10^{-2}	1	2×10^5
		2	8.3×10^5
Pressure gradient	2.4	1	2.5×10^5
		2	1.3×10^6

Table 4.4: Mesh refinement data without boundary layer refinement.

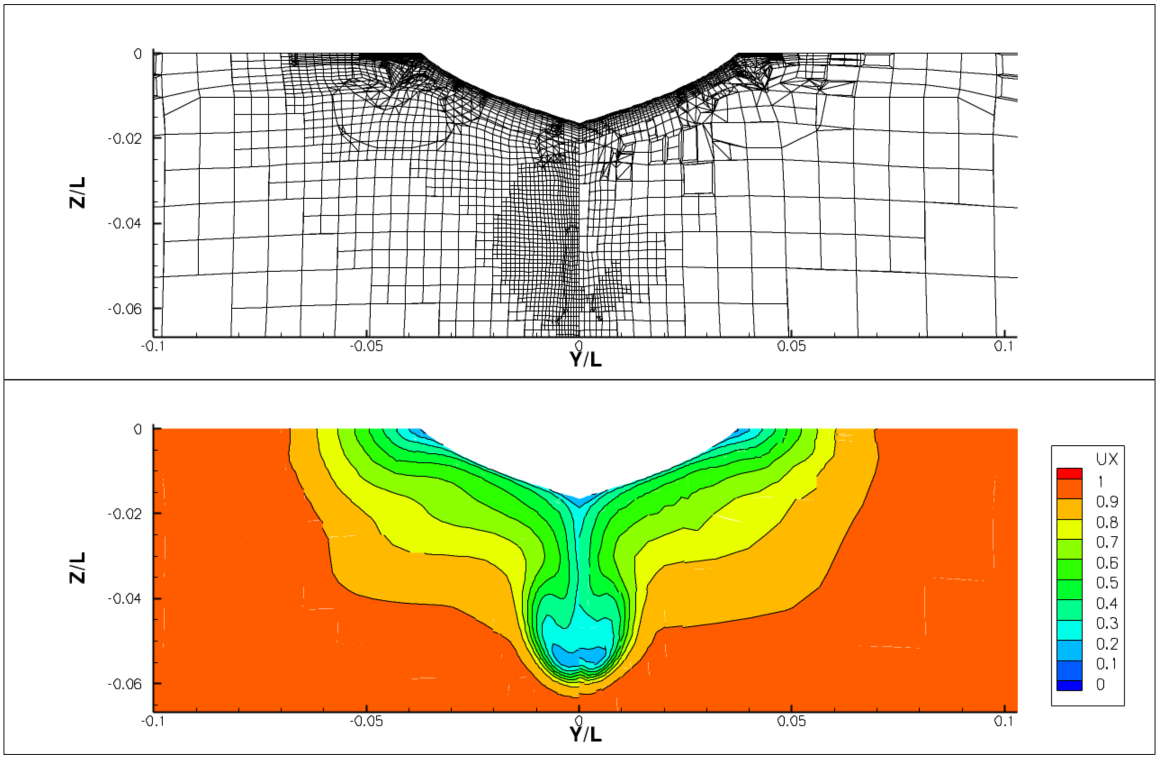

Figure 4.11: Velocity gradient criterion. Propeller plane Mesh and axial velocity contour. Mesh without boundary layer refinement on left and with boundary layer refinement on right.

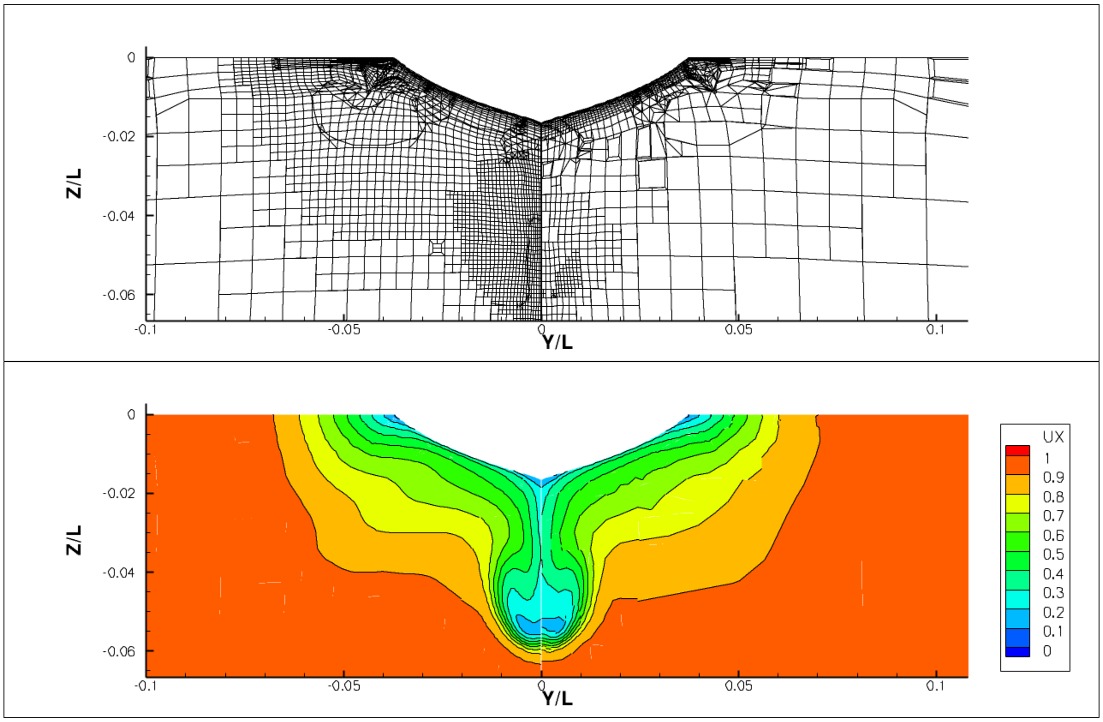

Figure 4.12: Vorticity criterion. Propeller plane Mesh and axial velocity contour. Mesh without boundary layer refinement on left and with boundary layer refinement on right.

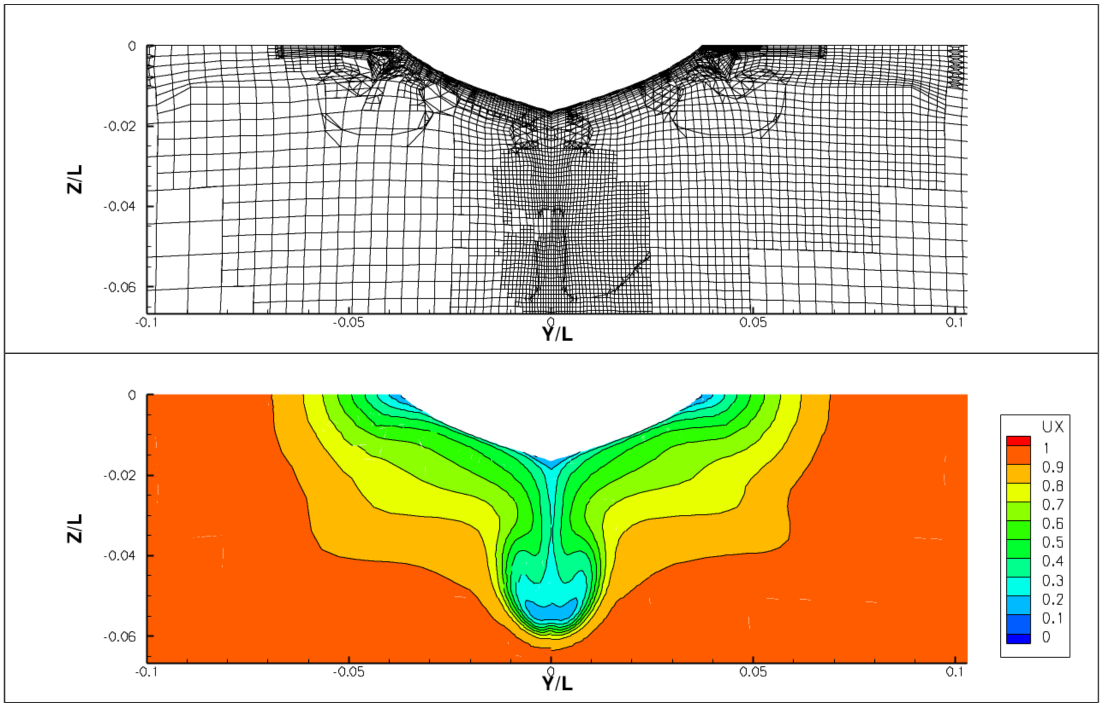

Figure 4.13: Pressure gradient criterion. Propeller plane Mesh and axial velocity contour. Mesh with boundary layer refinement on left and without boundary layer refinement on right.

4.3.3 Computations with EASM turbulence model

All the previous computations were performed using the k-ω SST turbulence model. Computations with Explicit Algebraic Stress Model (EASM) using the pressure gradient criteria are also performed. The cuts in the propeller plane, in figure 4.14, show that the pressure gradient criteria having the EASM model is better able to capture flow features specially the hook shaped low axial velocity zone found in experimental velocity profile as compared to the k-ω SST model.

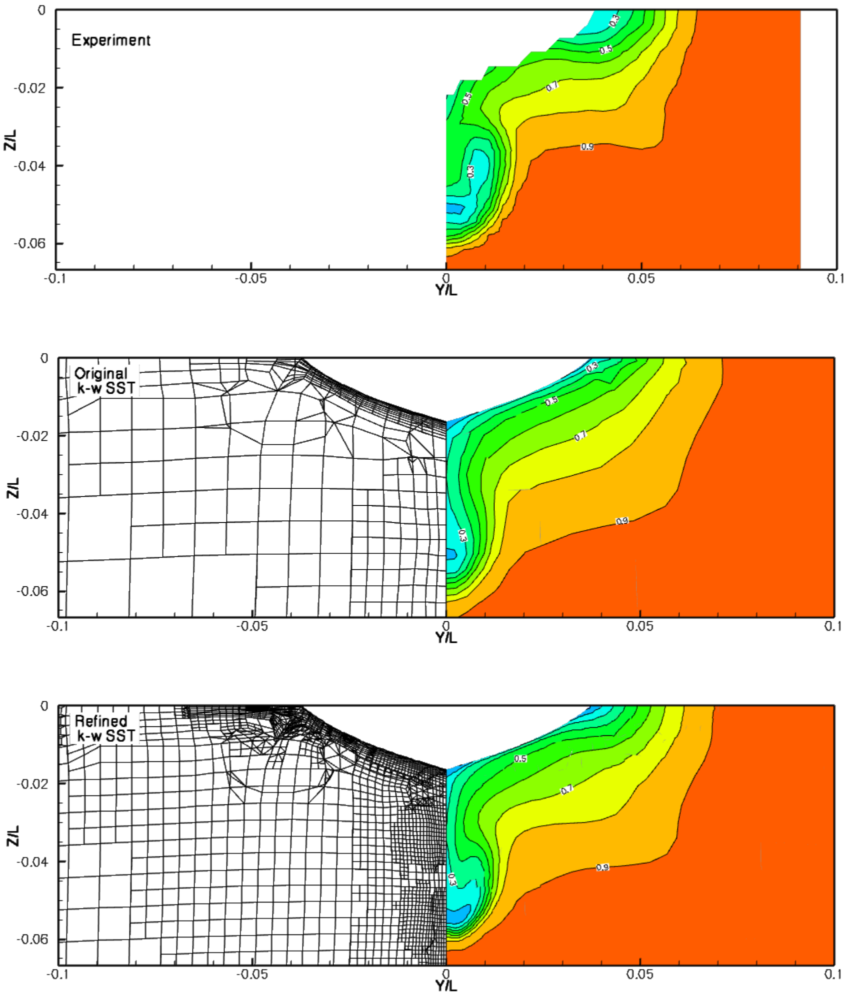

Figure 4.14: KVLCC2 tanker, cuts in the propeller plane. Grid cross-sections and axial velocity isolines are shown on the original coarse grid (5.8×10^3 cells) and the refined grids for the k-ω SST model (8×10^3 cells) and the EASM model (1.07×10^6 cells). The isolines are compared with measurements.

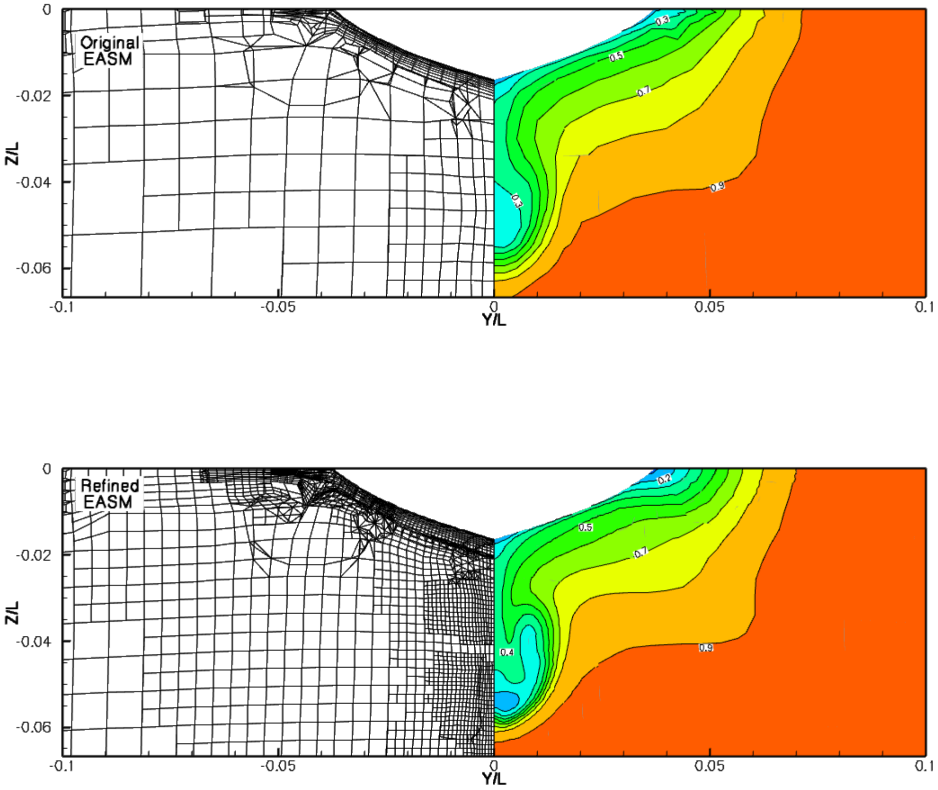

Figure 4.14 (continued): KVLCC2 tanker, cuts in the propeller plane. Grid cross-sections and axial velocity isolines are shown on the original coarse grid (5.8×10^3 cells) and the refined grids for the k-ω SST model (8×10^3 cells) and the EASM model (1.07×10^6 cells). The isolines are compared with measurements.

5 The NACA 16020 at incidence

The refinement criteria were tested, in the previous section, by computing the flow around a ship and analyzing the performance of these criteria in capturing the bilge vortices of the ship. It was found that the pressure gradient criterion has shown its superiority over the other two criteria. The effect of the boundary layer refinement was also noted. In this section we continue with the evaluation of the criteria performance by using another interesting test case which deals with accurate capturing of tip vortices of an aircraft wing.

Wingtip vortices are created when high-pressure air spills up over the wing tips into the low-pressure space above the wing as the aircraft generates lift. The cores of the vortices spin at very high speed and are regions of low pressure. Wingtip vortices are associated with induced drag and contribute to wake turbulence as well. The take off and landing of heavy aircraft produce severe wingtip vortices and a small light aircraft flying in such a vortex zone may be rolled over causing problems.

The effort in this section is the prediction of vortex core and the trajectory of the vortex using the refinement criteria. Computations are performed using various refinement threshold values and number of generations. As we will see later, that the boundary layer refinement is a dominant factor in determining the performance of the refinement criteria, as was the case in ship computations as well.

5.1 Mesh and numerical conditions

We focus here on the **NACA 16020** cross section configuration with a 10^0 incidence angle and a free-stream value of $U_{ref} = 10\ m/s$ as shown in figure 5.1. The maximum cord is $C_{max} = 0.475\ m$ and the length $L = 0.7125\ m$. For the considered velocity of $U_{ref} = 10\ m/s$, the Reynolds number based on C_{max} is $Re = 5.19 \times 10^6$ [5]. The mesh generation uses HEXPRESS^{TM}, an automatic full hexahedral meshing program developed by NUMECA. The wing is embedded in a rectangular box whose size is $[-1.5m,\ 3.5\text{m}] \times [-1.5m,\ 1.5\text{m}] \times [0m,\ 1.5\ m]$. Then, grid generation proceeds with mesh adaptation step to account for solid boundaries, refinement, trimming and snapping. At this step, a fully valid body fitted hex grid is generated. Then, viscous layers can be inserted and generated from user defined criteria: number of layers, stretching factor, and thickness of the first layer. Here we have addition of 30 viscous layers near the wall. Initially a coarse mesh is generated with approximately 0.5 million cells and then the refinement criteria are allowed to create a fine mesh. Grid refinement is limited to a box with dimensions $[0m,\ 1.5\text{m}]\times[-0.15m,\ 0.15\text{m}]\times[0.55m,\ 0.87\text{m}]$ in the computational domain to capture the vortex trajectory more accurately. The results are also available for a very fine mesh having approximately 4 million cells taken from the WP4 work package of the European VIRTUE project. This mesh and computational domain are shown in the figures 5.1 and 5.2.

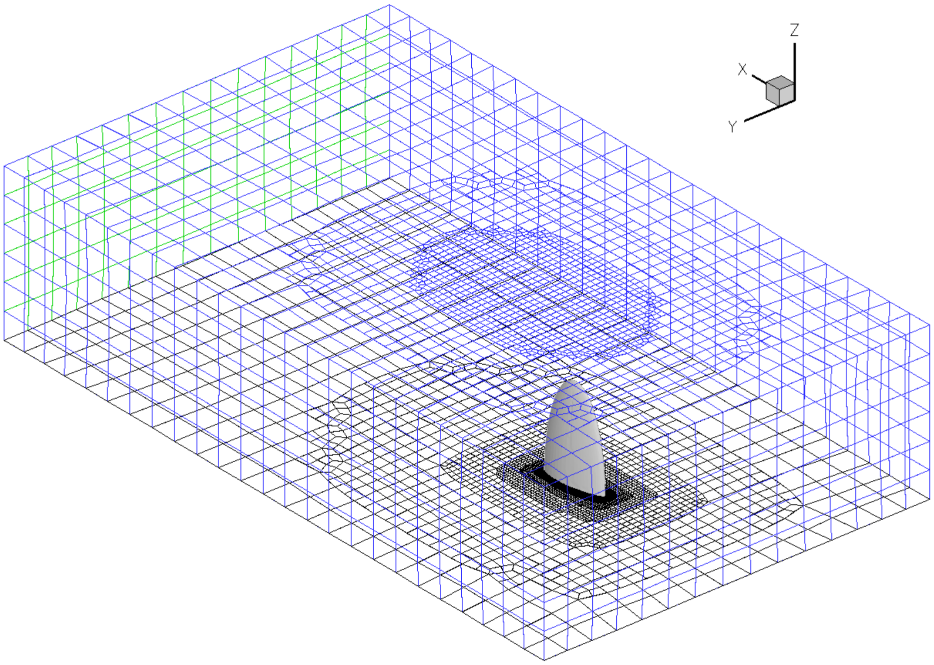

Figure 5.1: **NACA 16020** Computational domain- 4M cells.

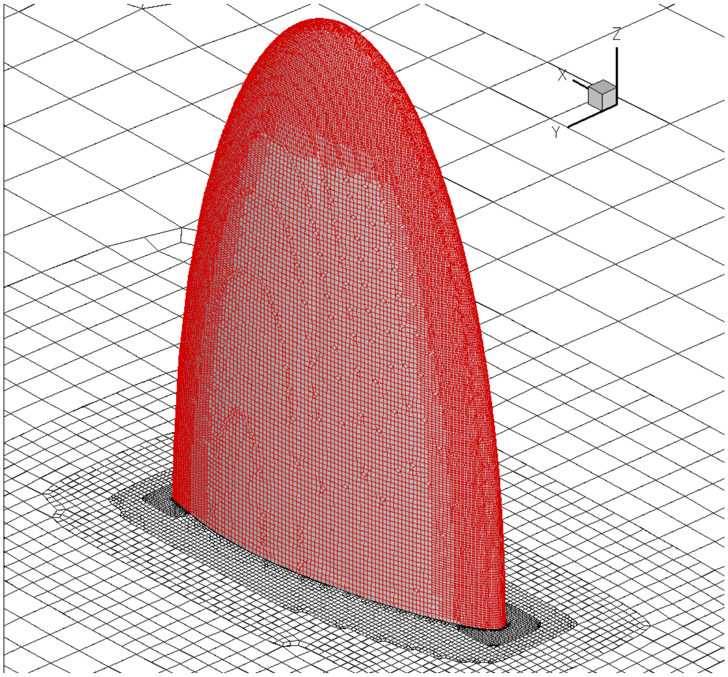

Figure 5.2: Surface mesh 4M cells.

5.2 Computations

All the computations were performed using an explicit algebraic turbulence stress model, EASM $k-\omega$, developed by ECN-CNRS [6]. This turbulence model has proved to be better than k-ω model for flow simulation around ships at full and model scale. Its degree of complexity is intermediate between a full Reynolds turbulence stress model and a classical isotropic model such as the $k-\omega$ SST model. Initially all the computations are performed with boundary layer refinement.

Threshold value	No of generations	No of cells after refinement
51	1	6.3×10^5
	2	6.4×10^5
	3	6.4×10^5
41	1	6.9×10^5
	2	7×10^5
	3	7.1×10^5
33	1	7.4×10^5
	2	8.4×10^5
	3	8.4×10^5

Table 5.1: Automatic grid refinement data for velocity gradient criterion

Threshold value	No of generations	No of cells after refinement
52	1	6.3×10^5
	2	6.4×10^5
	3	6.4×10^5
41	1	6.9×10^5
	2	7.1×10^5
	3	7.1×10^5
33	1	7.4×10^5
	2	8.1×10^5
	3	8.2×10^5

Table 5.2: Automatic grid refinement data for vorticity criterion

Threshold value	No of generations	No of cells after refinement
27	1	6.3×10^5
	2	7.8×10^5
9	1	7×10^5
	2	1×10^6
	3	1.8×10^6
5.7	1	8×10^5
	2	1.3×10^6

Table 5.3: Automatic grid refinement data for pressure gradient criterion

Criteria	Threshold value	Generations	Cells after refinement
Velocity gradient	2.5	2	7.6×10^5
Vorticity	11.5	2	8.3×10^5
Pressure gradient	8.5	2	7.4×10^5

Table 5.4: Automatic grid refinement data without boundary layer refinement

5.3 Results

The mesh and pressure contour plots for cross section at $X/C_{max} = 0.6$ are shown in figure 5.3 to 5.8 describing the performance of various refinement criteria in addition to initial and very refined grid results. As can be seen by the refinement criteria meshes, the velocity gradient and vorticity criteria have shown the same kind of behavior as in the KVLCC2 ship test case, i.e. refinement is dominant in the boundary layer region. Both criteria have proved inefficient for refining the area outside the boundary layer significantly, even with the lowest threshold value and maximum number of generations. On the other hand, if we look at the pressure gradient criteria we realize that even for the highest threshold value i.e. starting with the refinement of minimum number of cells, the vortex area has been identified and appreciable refinement has been done in that area.

A look at the data in tables 5.1 to 5.3 shows the same kind of saturation phenomenon as was shown by KVLCC2 test case; we see that for velocity gradient and vorticity criteria, the first two thresholds have very little increase in the grid size going from one number of generations to three. So for higher threshold values, the number of generations becomes insignificant. The pressure gradient criterion does not follow such trend and there is a significant increase in the number of cells if we increase the number of generations for a particular threshold value. The threshold value being very low in case of third threshold, allows the velocity gradient and vorticity criteria to refine the zones out of the boundary layer as well.

Some computations without boundary layer refinement are also performed and the results are shown in the figure 5.9 to 5.11. The performance of velocity gradient and vorticity criteria has improved this time with identification of the flow features and refining the zones outside the boundary layer while pressure gradient criteria does not behave normally as the vortex core is weaker due to generation of vortex inside the boundary layer.

Profiles of velocity and pressure corresponding to the vortex centre are presented in figures 5.12 to 5.14. The axial jet behavior is best reproduced by the pressure gradient criteria as compared to the other two (the velocity gradient and vorticity criteria without boundary layer refinement) and thus more axial speed gain is made by pressure criteria when compared to a very refined grid result. Tangential speed profile also follows the same trend. The peak pressure profiles also shows the superiority of the pressure gradient criteria

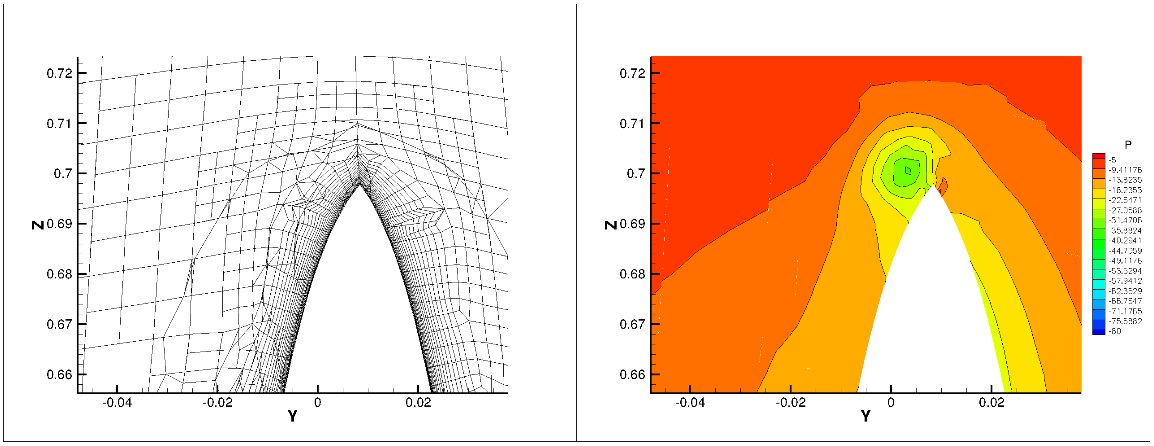

Figure 5.3: Original (0.5M cells) Mesh and pressure contour at $X/C_{max} = 0.6$

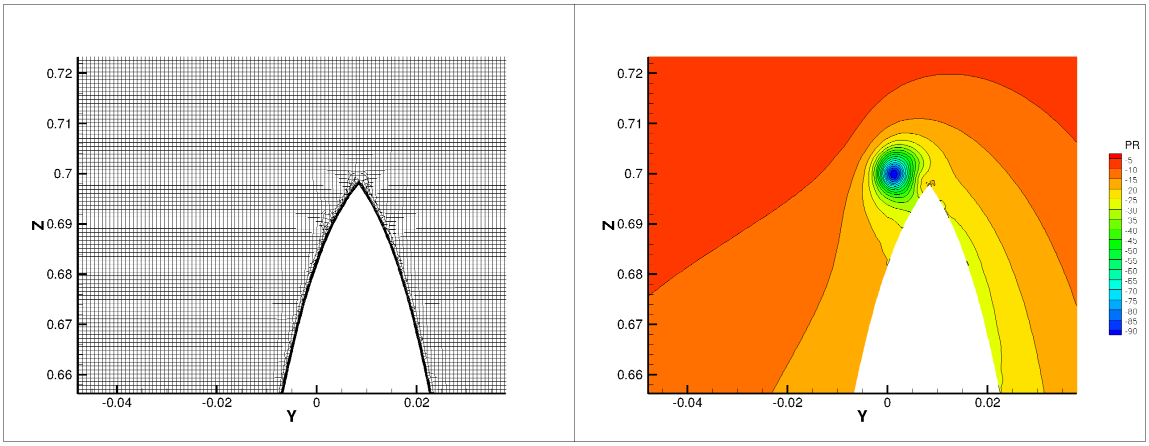

Figure 5.4: Uniformly refined (4M cells) Mesh and pressure contour at $X/C_{max} = 0.6$

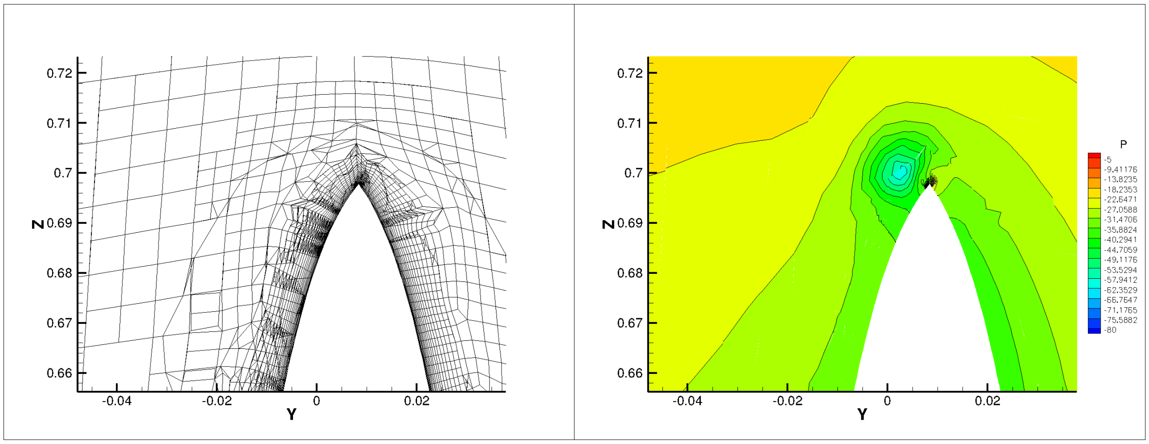

Figure 5.5: Velocity gradient criterion, Minimum threshold and 3 generations, Mesh and pressure contour at $X/C_{max} = 0.6$

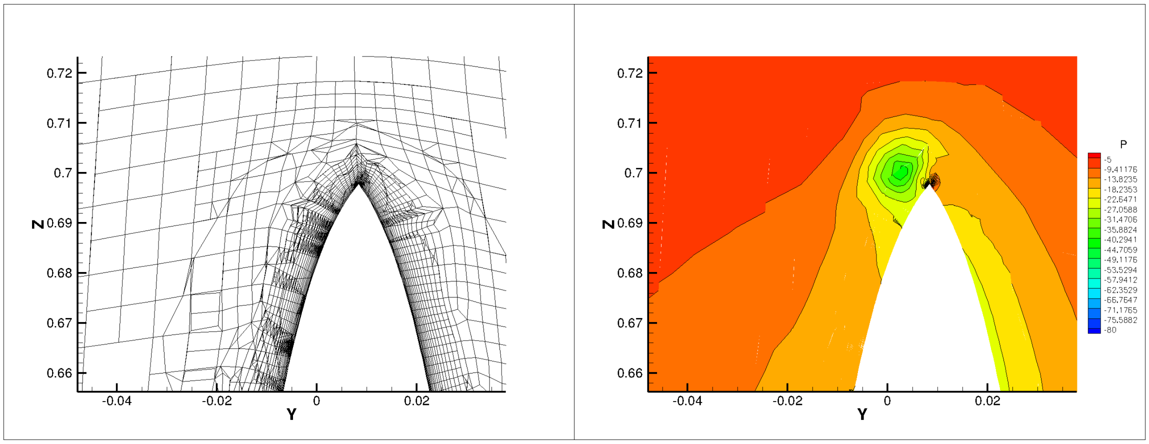

Figure 5.6: Vorticity criterion, Minimum threshold and 3 generations, Mesh and pressure contour at $X/C_{max} = 0.6$

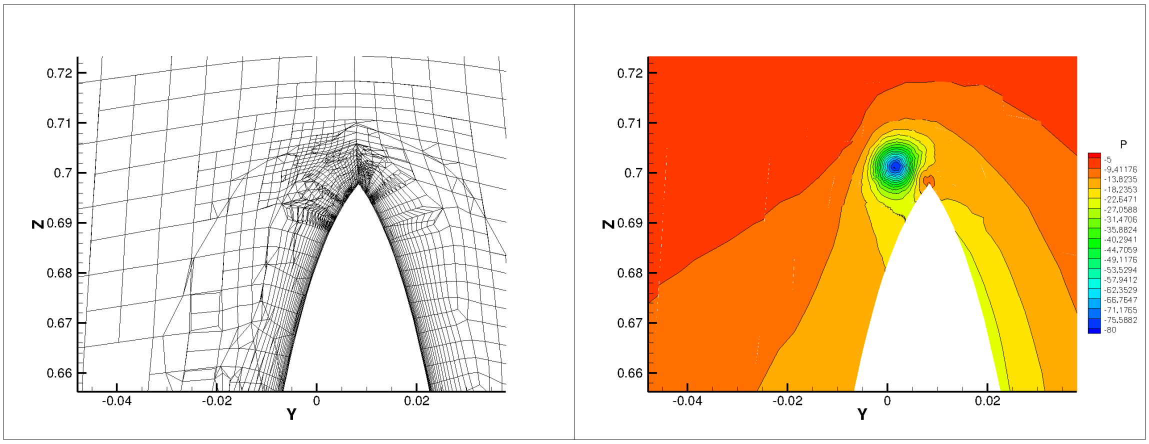

Figure 5.7: Pressure gradient criterion, Maximum threshold and 2 generations, Mesh and pressure contour at $X/C_{max} = 0.6$

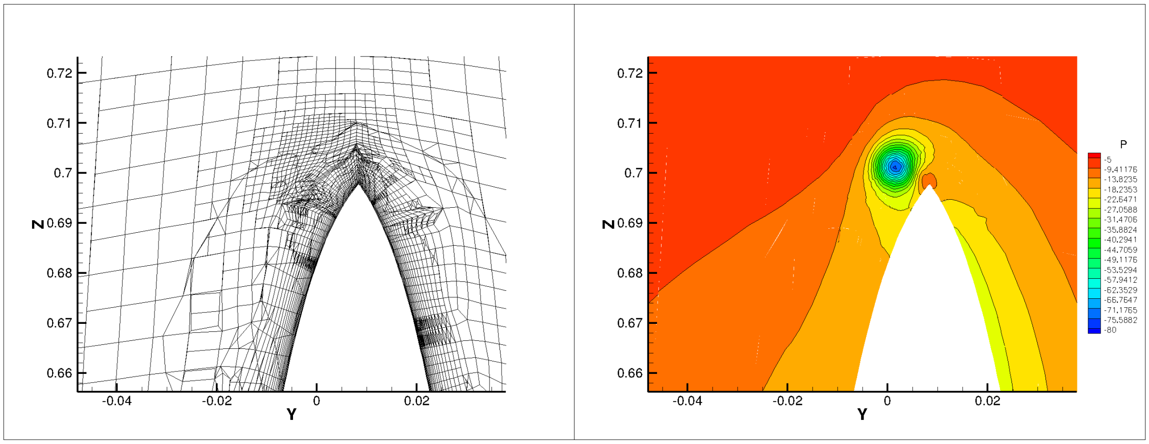

Figure 5.8: Pressure gradient criterion, Minimum threshold and 2 generations, Mesh and pressure contour at $X/C_{max} = 0.6$

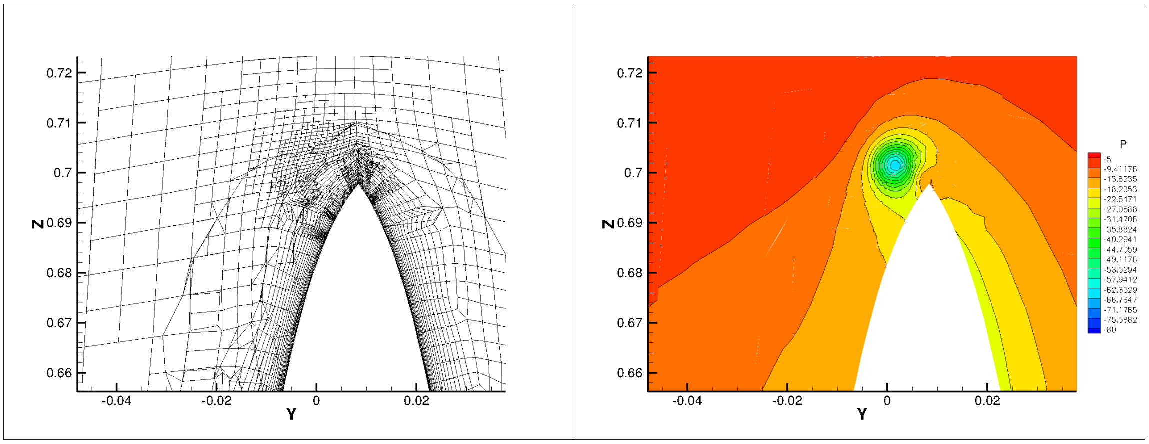

Figure 5.9: Velocity gradient criterion, without boundary layer refinement (0.7M cells with 2 generations) Mesh and pressure contour at $X/C_{max} = 0.6$.

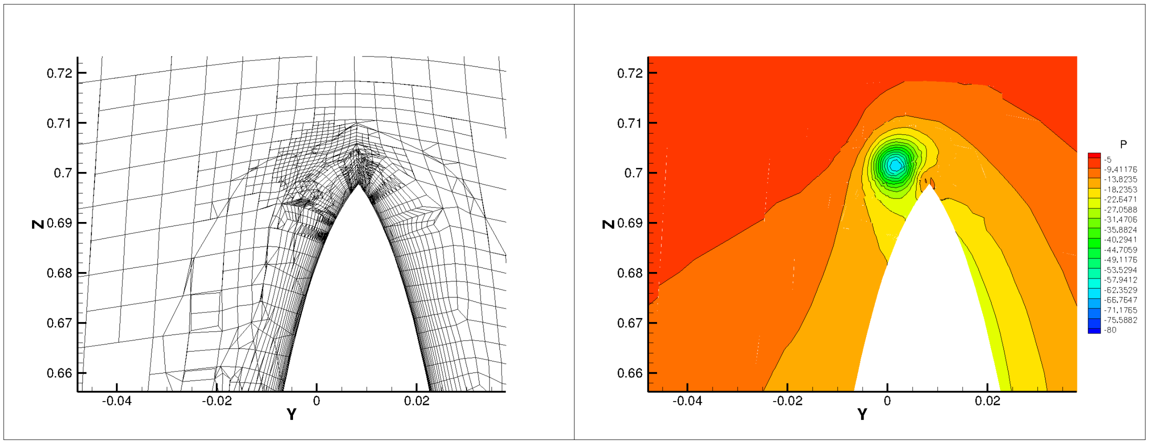

F

Figure 5.10: Vorticity criterion, without boundary layer refinement (0.8M cells with 2 generations) Mesh and pressure contour at $X/C_{max} = 0.6$.

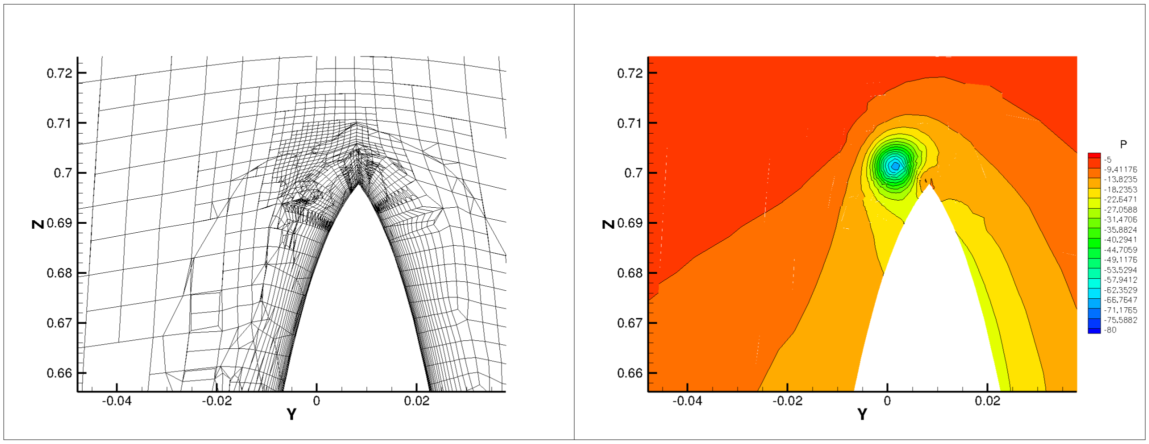

Figure 5.11: Pressure gradient criterion, without boundary layer refinement (0.7M cells with 2 generations) Mesh and pressure contour at $X/C_{max} = 0.6$.

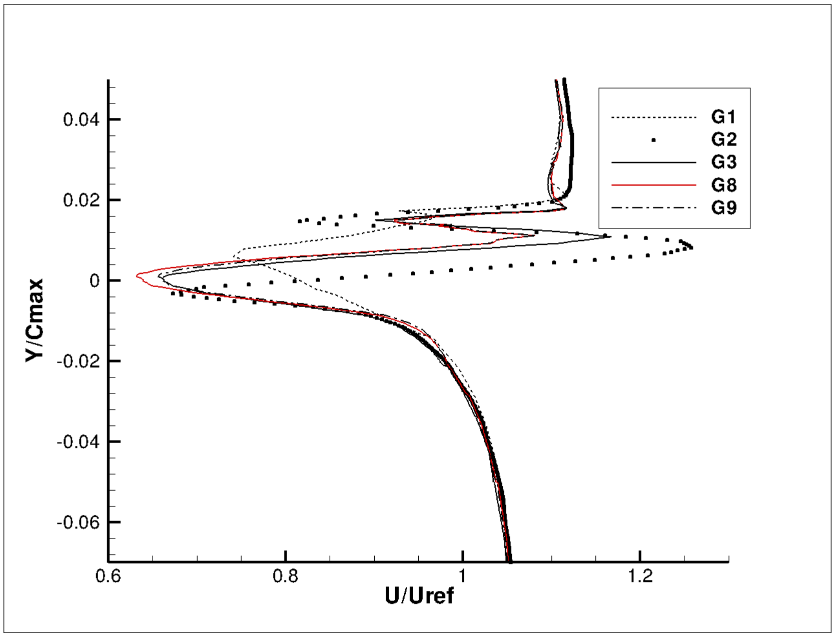

Figure 5.12: Axial velocity profile at X/C$_{max}$ = 0.6 (Legend G1 = Original coarse mesh, G2 = Uniform refined (4M cells) mesh, G3 = Pressure gradient criterion at minimum threshold and 2 generations, G8 = Velocity gradient criterion without BL refinement and 2 generations, G9 = Vorticity criterion without BL refinement and 2 generations).

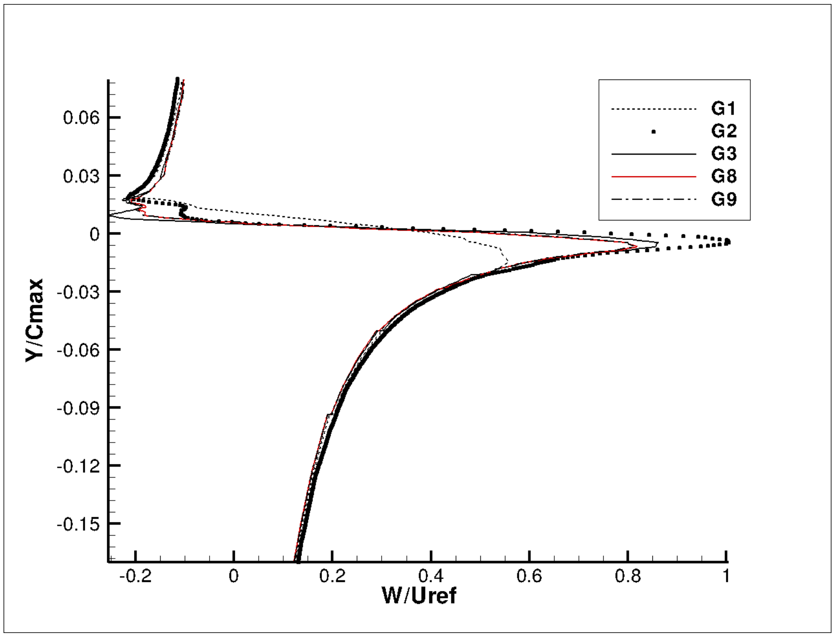

Figure 5.13:Tangential velocity profile at X/C$_{max}$ = 0.6 (Legend described in Figure 5.12).

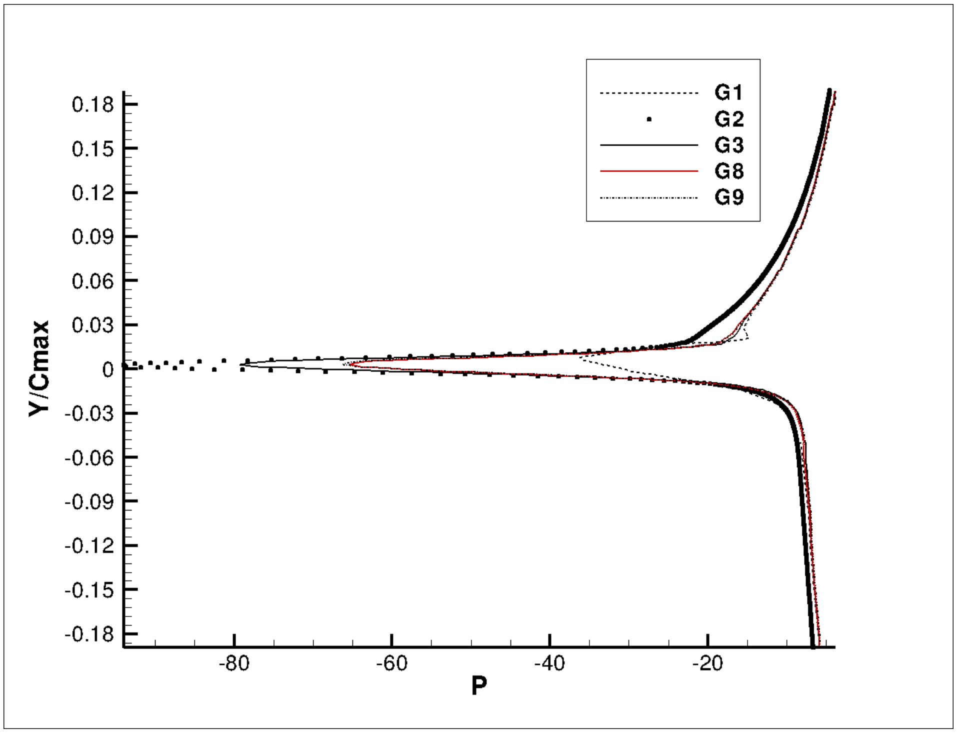

Figure 5.14: Pressure (KPa) profile at X/C_{max} = 0.6 (Legend described in Figure 5.12).

Conclusions

The use of grid adaptation allows having more accurate solutions with limited number of grid points. One of the concerns for adaptive grid refinement is the selection of adequate refinement criteria for minimizing analysis errors. The current project is a part of an effort to develop a series of refinement criteria for the adaptive grid refinement part of the ISIS-CFD flow solver. In this process, three error indicators or refinement criteria are chosen to be tested. These are based on the absolute value of pressure gradient, velocity gradient and vorticity.

A simple problem with a vortex flow in a cylinder was initially set to validate that the criteria were actually responding to the flow features and were identifying the zones for refinement leading to adaptive grid refinement. The criteria were tested using various threshold values and number of generations. Threshold values were selected on the basis of number of cells which should be initially marked for refinement or de-refinement. The criteria also showed better performance than the uniform grids in terms of human and computational costs as much less number of grid points is required to reach a desired accuracy in adaptive mesh refinement.

The next step was to check the performance of these criteria on two more complex test cases. The KVLCC2 test case and the NACA 16020 at incidence case were employed in this regards. It was noted that pressure gradient criteria performs best among the three criteria and is more general than the other two because it prevents the unnecessary and costly refinement in the boundary layer cells. The computations performed without boundary layer refinement depict that the performance of the velocity gradient and vorticity criteria improves significantly and is consistent with the behavior of the pressure gradient criterion.

There are many possibilities for further research as well. More time was consumed in the computations with boundary layer refinement and the computations without boundary layer refinement could not be analyzed in detail which could have lead to some other aspects of the refinement criteria performance. The refinement criteria were tested at very initial stages and more verification and validation is needed till such criteria could be used efficiently. The criteria are checked for single fluid flows initially, and are still to be tested on multi-fluid and free surface flows in particular. The refinement was isotropic in all the computations and it will be interesting to check how the criteria perform in directional refinement. Another possibility can be the application of such criteria to analyze vortex shedding in automotive flows and it will be interesting to see the performance of these criteria.

References

[1] P. Queutey and M. Visonneau. An interface capturing method for free-surface hydrodynamic flows. *Computers & Fluids*, **36**(9), 1481–1510, (2007).

[2] A. Hay. *A study of numerical error estimation and local adaptive unstructured mesh refinement strategies for the Reynolds Averaged Navier-Stokes equations*, Ph.D. thesis, University of Nantes, France, February 2004.

[3] J. Wackers and M. Visonneau. *Adaptive grid refinement for ISIS-CFD*, 11th Numerical Towing Tank Symposium (NuTTS 2008), Landéda, France.

[4] L. Larsson, F. Stern, and V. Bertram, editors. Gothenburg 2000, *A Workshop on Numerical Ship Hydrodynamics*. Gothenburg, Sweden, 2000.

[5] D. Dauby. *Simulation of cavitating flows by resolution of the Reynolds Averaged Navier-Stokes equations. Application to tip-vortex cavitation,* Ph.D thesis, University of Nantes, France, 2004.

[6] G.B. Deng, R. Duvigneau, P. Queutey and M. Visonneau, *Assessment of turbulence model for ship flow at full scale*, Comp. Mech., WCCM IV, Beijing, China, September 2004.

[7] *www.cfd-online.com/Wiki/Meshing*